Traditional irrigation practices sustain groundwater quality in a semiarid piedmont

H. Bouimouass, Y. Fakir, Sarah Tweed, H. Sahraoui, M. Leblanc, A. Chehbouni

▶ **To cite this version:**

H. Bouimouass, Y. Fakir, Sarah Tweed, H. Sahraoui, M. Leblanc, et al.. Traditional irrigation practices sustain groundwater quality in a semiarid piedmont. CATENA, 2022, 210, pp.105923. 10.1016/j.catena.2021.105923 . hal-03740198

HAL Id: hal-03740198
https://hal.inrae.fr/hal-03740198

Submitted on 5 Jan 2024

HAL is a multi-disciplinary open access archive for the deposit and dissemination of scientific research documents, whether they are published or not. The documents may come from teaching and research institutions in France or abroad, or from public or private research centers.

L'archive ouverte pluridisciplinaire **HAL**, est destinée au dépôt et à la diffusion de documents scientifiques de niveau recherche, publiés ou non, émanant des établissements d'enseignement et de recherche français ou étrangers, des laboratoires publics ou privés.

Distributed under a Creative Commons Attribution - NonCommercial 4.0 International License

Version of Record: https://www.sciencedirect.com/science/article/pii/S0341816221007815
Manuscript_480ce0fa76e31d440265cfeb6d16fbdc

Traditional irrigation practices sustain groundwater quality in a semiarid piedmont

H. Bouimouass[1,*], Y. Fakir[2,3], S. Tweed[4], H. Sahraoui[1,2], M. Leblanc[1,3,5], A. Chehbouni[3,5,6]

[1] Hydrogeology Laboratory, UMR EMMAH, [2]University of Avignon, Avignon 84000, France
[2] Department of Geology, Faculty of Sciences–Semlalia, Cadi Ayyad University, Marrakech 40001, Morocco.
[3]CRSA (center for remote sensing application), UM6P, Benguerir 43150, Morocco
[4]UMR G-EAU, IRD, Montpellier 34090, France
[5]IWRI (international water research institute), UM6P, Benguerir 43150, Morocco.
[6]CESBIO (centre d'études spatiales de la biosphère), Toulouse 31400, France

*Corresponding author at: Department of Geology, Faculty of Sciences–Semlalia, Cadi Ayyad University, P.O. Box: 2390, 40001 Marrakech, Morocco.
E-mail address: Bouimouass.h@gmail.com (H. Bouimouass)

© 2021 published by Elsevier. This manuscript is made available under the CC BY NC user license
https://creativecommons.org/licenses/by-nc/4.0/

Abstract

In semi-arid areas, agricultural practices have been found to significantly alter groundwater quality. Although significant research has been conducted on the impacts of the intensification of irrigated agriculture, many pivotal questions remain relating to the impact of traditional agricultural practices on groundwater quality. In this study, the results of major ions analysis of 91 water samples collected in the semi-arid piedmont of the High Atlas Mountains, central Morocco, are used to assess the impact of traditional irrigation practices on groundwater quality. Despite the use of organic fertilizer in the irrigated area, the NO_3 groundwater concentrations remain low (median = 9 mg/L) and only increase on average by 3.6 mg/L during the irrigation season. All groundwater sampled in the irrigation area has an excellent quality for both drinking and irrigation purposes based on the chemical indices. Overall, groundwater chemistry is controlled by geogenic processes. Relationships between major ion in groundwater reflects the mineral dissolution and ion exchange processes during the trajectory of the streamwaters from the mountain to the alluvial plain via irrigation practices. In comparison, in the non-irrigated area, halite dissolution and/or transpiration processes results in increases in electrical conductivity values that were over twice the values in the irrigated area. The seasonal decrease of electrical conductivity values in groundwater beneath the irrigated area (on average from 841 to 692 µS/cm) is a result of irrigation recharge, which counterbalances effects of salinization mechanisms that can often characterize irrigated arid zones. These results highlight the low impacts of this ancestral hydro-agro system on groundwater quality. Such a traditional irrigation system provides a nexus between food production, low energy costs (streamflow diversions by gravity-fed channels), and low environmental impacts. In the context of accelerations in global change impacts via the rapidly expanding modern irrigation practices, such traditional hydro-agro systems, where possible, should be highlighted and preserved.

Keywords: Traditional agriculture, alluvial aquifer, hydrochemistry, water-rock interaction, ion exchange.

1. Introduction

Agricultural practices have significantly altered groundwater quality (Foster and Chilton, 2003; Duncan et al., 2008; Foster et al., 2018). This is a worldwide issue, and has been documented in many countries including in Uzbekistan (Johansson et al., 2009), Spain (Merchán et al., 2015; 2020), France (e.g. Tweed et al., 2018), Japan (Nakagawa et al., 2021), China (Zhang et al., 2012; Hu et al., 2019), and Tunisia (Haj-Amor et al., 2017). In particular, the transition from non- or traditionally-irrigated areas to the expansion and intensification of modern irrigation practices has had significant impacts on the deterioration of groundwater quality (Scanlon et al., 2007). Areas equipped with modern irrigation techniques and destined for intensive agricultural exploitation have globally increased from 170 to 333 Mha between 1965 and 2015 (FAO and IWMI, 2018). Keeping in mind that many rural areas around the world use groundwater for domestic purposes without any treatment (Ravindra and Garg, 2007; Buschmann et al., 2008; Coyte et al., 2019), actions are required to protect groundwater quality from impacts of these irrigation expansions. This is particularly the case for alluvial aquifers, which can provide important water supplies (Mvandaba et al., 2018; Xiao et al., 2021), but at the same time are also typically vulnerable to pollution (Wu and Sun, 2016).

Significant progress has been made in identifying the controlling processes of groundwater quality deterioration in irrigation areas (Xiao et al., 2020), which includes both geogenic and anthropogenic influences. Whilst some studies have found that irrigation by surface waters has increased groundwater salinity (Rabemenana et al., 2005; Scanlon et al., 2007), others have found irrigation by low salinity surface water has buffered groundwater from salinization impacts (Stigter et al., 2006; Rotiroti et al., 2019; Jia et al., 2020). Irrigation with diverted surface waters can result in groundwater mounds due to increased recharge. This recharge and rise in the water table can result in more rapid vertical transfers of agricultural chemicals from the surface to the saturated zone (Elmeknassi et al., 2021; Nakagawa et al., 2021), mobilization of evaporites from the unsaturated zone (Durhan et al., 2008), and an increase in the evaporative effects on the concentrations of contaminants in the shallow groundwater (Cartwright et al., 2007; Scanlon et al., 2007), especially under semi-arid climates. In addition, where the surface water used to irrigate is of poor quality, and the hydrogeological conditions allow for rapid infiltration of contaminants that remain mobile (Xiao et al., 2017), the recharge of irrigation waters can result in the widespread transfer of surface contaminants to the aquifer (Exner et al., 2014; Juntakut et al., 2019). This is particularly observed in agricultural regions located down-gradient from cities that are either

heavily populated, have high runoff events, and/or have poor infrastructure to treat wastewater from domestic and industrial zones before flowing into the connecting rivers (Li et al., 2016; Panda et al., 2018; Liu et al., 2020).

The majority of the studies regarding the impact of irrigation on groundwater quality have considered the effects of modern irrigation systems, such as drip irrigation and cross-regional transfers (Chen and He, 2003; Jia et al., 2020). In comparison, fewer research has focused on traditional irrigation systems, such as streamflow diversion by traditional irrigation channels called Seguias (Bouimouass et al., 2020) or Acequia (Fernald et al., 2015; Turner et al., 2016). In semi-arid zones, streamflow diversion by traditional irrigation channels is common in irrigated areas adjacent to mountain ranges. Mountains are water towers for the adjacent lowlands because they receive more precipitation due to the orographic effect, and the accumulation of snow and ice contribute to runoff during hot and dry seasons (Immerzeel et al., 2020). Mountain streamflow sustains the downstream areas (Viviroli et al. 2007; Immerzeel et al. 2010) and a recent study showed that almost 1.5 billion people will depend on water contributions from mountain areas by the mid-twenty-first century (Viviroli et al., 2020). However, mountains are highly sensitive to climate and anthropogenic changes (Viviroli et al., 2011, Hock et al., 2019; Immerzeel et al., 2020). With worldwide decreases in snow already observed over the last decades (Berghuijs et al., 2014; Malek et al., 2020; Immerzeel et al., 2020), and decreases forecasted under climate change (Marchane et al., 2015; Baba et al., 2018; Hajhouji et al., 2020; Immerzeel et al., 2020; Viviroli et al., 2020), traditional irrigation areas and related groundwater renewal processes will be affected.

In traditional irrigation areas, particularly in semi-arid regions, flood irrigation is often an important source of groundwater recharge (Foster and Perry, 2009; Jimenez-Martinez et al., 2009; Bresciani et al., 2018; Rotiroti et al., 2019; Bouimouass et al., 2020). This recharge has also been found to improve groundwater quality, for example via the dilution of groundwater salinity (Rotiroti et al., 2019). In contrast, Juntakut et al., (2019) found that traditional gravity-fed irrigation resulted in greater nitrate concentrations in groundwater compared with center pivot-irrigation systems. Further investigation and characterization of groundwater quality under such traditional irrigation practices, in the context of climate change and population growth, is critical for water resources especially in semi-arid regions.

In the piedmont of the High-Atlas Mountains in the semi-arid Haouz plain, central Morocco, traditional irrigation is the main groundwater recharge source (Bouimouass et al., 2020). The area preserves a traditional agriculture where local small-scale farms have limited

use of organic fertilizers for growing wheat and olives trees, irrigated by diverting the streamflow of the High-Atlas Mountains via channels known as Seguias. Groundwater from the alluvial aquifer is the sole drinking water resource for this rural area and it is used without any treatment. In this study area, we investigate the impacts of irrigation water recharge on groundwater quality via the evolution of salinity, nitrate and major ion concentrations in waters from the high elevation mountains to the piedmont. The results are used to determine whether the current traditional irrigation practices provide a model for sustainable agricultural practices and groundwater resources for a semi-arid region.

2. Study area

2.1. Location, climate and hydrology

As is the case for the whole of North Africa, Morocco is characterized by an arid to semi-arid climate with high inter-annual variability and several periods of below average precipitation (Jarlan et al., 2016). Piedmont areas along the High-Atlas in Morocco benefit from a milder climate and from streamflow generated at high altitudes (Toubkal peak at 4167m) by rainfall and snowmelt. The study area is crossed by the Ourika stream and extends from the High-Atlas Mountains to the edges of the Haouz plain, in central Morocco (Fig. 1). The Ourika stream, which drains a watershed in the High-Atlas of 492 km^2, is one of the main tributaries of the Tensift basin (Fig. 1). The climate varies from arid to semiarid in the plain, and from semiarid to sub-humid in the High Atlas Mountains. The mean annual rainfall ranges from 200 mm in the plain to 600 mm in the mountains as both rain and snow. In the High-Atlas Mountains, streams are fed by rainfall and snowmelt (Marchane et al., 2015; Hajhouji et al., 2018). The snowmelt contributes on average 15% to 30% of the streamflow (Boudhar et al. 2009; Boudhar et al., 2016). Therefore, the streamflow is high during winter and spring and low during summer and autumn. The average inter-annual flow-rate of the Ourika stream is 4.92 m^3/s at the Aghbalou gauging station (Fig. 1).

2.2. Geology and hydrogeology

The High-Atlas mountains extend from Morocco to Tunisia, the highest part is the High-Atlas of Marrakech encompassing the study area. The High-Atlas of Marrakech is characterized by a heterogeneous bedrock (Fig. 2), involving complex lithological and structural variations (Delcaillau et al., 2011). The upper part of the High-Atlas Mountains is dominated by a massif of Precambrian granodiorite rich silicates such as plagioclase and amphibole (Juery, 1976). The middle part is formed of Triassic and Visean sandstone and siltstone. The lower part of the High-Atlas, overlooking the piedmont area, is characterized by

161 the presence of Triassic conglomerate, red sandstone, silt and clay containing evaporite
162 mineral deposits, topped by infraliassic basalts, and by Eocene limestone and conglomerates
163 of Mio-pleocene (Ouanaimi, 2011). The piedmont is formed of Neogene and Quaternary
164 alluvial deposits that extend northward over the Haouz plain. They represent the main aquifer.

165 The piedmont area of the High-Atlas in the Tensift basin contains a large unconfined
166 aquifer and two confined aquifers (with very limited spatial extent). The unconfined aquifer in
167 the Haouz plain consists of alluvial fans and fluviatile deposits of Neogene and Quaternary
168 age. The aquifer covers almost 6000 km^2 and it constitutes the principal groundwater resource
169 of the Haouz plain. It is characterized by a heterogeneous transmissivity varying from $5x10^{-5}$
170 to $9x10^{-2}$ m^2s^{-1} with an average of $6.7x10^{-3}$ m^2s^{-1} (Sinan and Razack, 2006). The unconfined
171 aquifers are encompassed in the Eocene and the Turonian–Cenomanian limestone. Little
172 knowledge is available on the hydrogeological characteristics of these aquifers characterized
173 by high spatial heterogeneity. In the study area, belonging to central Haouz, the Neogene and
174 Quaternary alluvial fan are as thick as 50 m, followed by a thick basement up to 121 m
175 consisting of Miocene clay and marls (Sinan, 2000). The Eocene confined aquifer consists of
176 100 m of limestone, followed by a 60 m of impermeable marls and red sandstone (Sinan,
177 1986). The second confined aquifer of Turonian–Cenomanian limestone is 45 m thick lying
178 above a 50 m of Cenomanian clay forming its basement (Sinan, 2000). The present study
179 targeted the alluvial aquifer where groundwater levels can raise to up to 4 m during wet
180 season in the riparian zone and be as deep as 50 m away from the Ourika wadi (Bouimouass
181 et al., 2020). From the dry season to the wet season, groundwater levels substantially increase
182 due to recharge by in-channel streamflow losses and mainly by surface water irrigation
183 (Bouimouass et al., 2020).

184 **2.3. Land and water use**

185 Human settlements in the study area are in form of small villages with population often
186 not exceeding 200 person and are dispersed all over the rural area, except for some towns
187 where population can be of several thousand persons (Fig. 1). These small settlements use
188 septic tanks (up to 5 m) for their domestic wastes which are potentially threating groundwater
189 quality especially where the aquifer is shallow. Since hundreds of years, the area hosts
190 traditional agricultural practices, consisting of a subsidence production system composed
191 mainly of olive trees (Fig. 3A) and wheat. This traditional agriculture has been secularly
192 irrigated by a large network of gravity-fed surface irrigation earth channels (locally named
193 Seguias) that divert the streamflow (Fig. 3B, C, D and E). This hydro-agro-system is similar

194 to the so-called spate irrigated systems, which are particularly found in areas where mountain
195 catchments border lowlands, in the Middle East, North Africa, West Asia, East Africa and
196 parts of Latin America (Van Steenbergen et al., 2011). This type of traditional irrigation is
197 used to expand irrigation from the piedmont to the plain. During the last century, after the
198 French colonization in Morocco, this type of traditional irrigation on the plains has been
199 increasingly replaced by modernized agriculture, as it is the case for most of the plains around
200 the world (Scanlon et al., 2007), with resultant impacts on groundwater quality and quantity
201 (Hu et al., 2019). Nowadays, traditional irrigation is largely restricted to piedmont areas.

202 The study area offers the possibility of investigating two areas of contrasting land and
203 water use. The western side of the Ourika wadi is characterized by extended cultivable lands
204 irrigated by the streamflow that is diverted via the network of irrigation channels (Fig. 1). In
205 comparison, the eastern side of the Ourika wadi is crossed by few irrigation channels, and
206 crops depend mainly on rain-fed irrigation. In this study, we refer to these two areas as
207 irrigation and non-irrigation areas respectively.

208 ## 3. Material and methods

209 ### 3.1. Sampling and analyses

210 In this study major ion data of precipitation, surface water, springs and groundwater are
211 compared. Precipitation (n=8) were collected in three different elevations spanning the plain,
212 piedmont and high elevations during November 2017 and February 2018. Surface water
213 (n=12) and mountain groundwater (n=12) were collected in two sites in Ourika wadi and two
214 springs with different elevations at a monthly basis from September 2017 to March 2018
215 (except for October 2017). Groundwater (n=55) collected from 27 wells were sampled during
216 four field campaigns in September 2017, November 2017, December 2017 and March 2018.
217 Sampling locations are presented in Figure 1. The sampling sites were chosen as private
218 irrigation and domestic supply wells spanning different land use (irrigated area, non-irrigated
219 area), with depth ranging from 12 to 50 m pumping water from the phreatic aquifer. Some
220 wells were sampled multiple times depending on access. Samples were collected during or
221 immediately after pumping for irrigation and conserved in 300 ml high-density polyethylene
222 bottles and preserved cold until analysis.

223 The physical parameters (temperature, pH, and EC) were measured in the field using a
224 portable pH meter sension+ for pH (Hach) and temperature and a portable conductivity meter
225 for EC (Hanna instruments). All samples were analyzed for cations (Ca^{2+}, Na^{+}, Mg^{2+}, K^{+})
226 after being filtered at 0.45 µm and acidified with HNO_3 and anions (Cl^{-}, SO_4^{2-}, NO_3^{-}) using

ion chromatography (Dionex; ICS1100 and autosampler AS-AP) at the laboratory of Hydrogeology of Avignon University. The alkalinity was measured using a HACH digital titrator at the end of the day. Triplicate analyses for each sample were used to assess the analysis uncertainty and the relative standard deviations was around 3%. The quality of water analyses is assessed using the charge balance error (CBE). Water samples having a higher concentration of cations show positive CBE, while negative CBE is credited to higher concentrations of anions (Bozdag et al., 2015). CBE was computed by Equation (1);

$$\%CBE = \frac{[\sum cations - \sum anions]}{[\sum cations + \sum anions]} \times 100 \quad (1)$$

where ionic concentrations are expressed in milliequivalent per liter. According to the standard protocols, only those water samples were accepted that had less than ±5% CBE (Xiao et al., 2021).

3.2. Water suitability for domestic and irrigation uses

Major ions and physiochemical parameters have long been recognized as important indicators for water quality (Vaiphei and Kurakalva, 2021). Common parameters include electrical conductivity (EC) as a measure of salinity (Thorslund and Vliet, 2020; Banna et al., 2014), pH to monitor acidity levels of drinking water (Vaiphei and Kurakalva, 2021), nitrogen species as an indicator of the impacts of agricultural activities on groundwater (Teng et al., 2019), and other major ions such as sodium and chloride that have be used to detect seawater intrusion, evaporate dissolution, and fertiliser contamination (Bresciani et al., 2018; Rajmohan et al., 2021). Such indicators of water quality are valuable in that they are relatively easy and cheap to measure, and are therefore ideal to monitor water quality across regional and remote hydrogeological basins and/or over long timeframes. In order to analyse the information provided by these physiochemical parameters, water quality indices have been established based on different statistical methods (Simões et al., 2008; Sun et al., 2016). Some of the most widely used water indices used in irrigation areas are the sodium adsorption ratio (SAR), residual sodium carbonates (RSC), sodium percentage (% Na) and Kelly's ratio (KR) (Kelly, 1993; Vincy et al., 2015). These indices have been widely used and proven to be effective in assessing and monitoring groundwater quality (Celestino et al., 2019; Talib et al., 2019; Xu et al., 2019).

The water quality index was also used in this study to analyse potential impacts of irrigation in the groundwater resource quality. This is a widely used tool to assess the suitability of groundwater for drinking supplies (Talib et al., 2019). The WQI relies on the

concentrations and the weight coefficient of the chemical elements. The coefficients are based on the impact of each element on the human health (Xiao et al., 2019). The WQI is calculated according to the following equation:

$$WQI = \sum[W_i \times \left(\frac{C_i}{S_i}\right) \times 100] \quad (2)$$

Where C_i is the concentration of each parameter, S_i is the corresponding standard WHO values (WHO, 2017) and W_i is the relative weight of each parameter computed following the equation:

$$W_i = \frac{w_i}{\sum_{i=1}^{n} w_i} \quad (3)$$

Where w_i is the weight of each parameter and n is the number of parameters. Table 1 shows the relative S_i and W_i for each parameter used (Talib et al., 2019).

Nitrate (NO_3^-) concentrations were also used in this study as an indicator of groundwater contamination by leaching of (mineral and organic) fertilizers or septic waste, as they are important for health concerns (WHO, 2011).

Similar to drinking water, there are several indices used to assess the suitability of groundwater and surface water for irrigation (Talib et al., 2019; Xu et al., 2019; Xiao et al., 2020). The indices sodium adsorption ratio (SAR), residual sodium carbonates (RSC), sodium percentage (% Na) and Kelly's ratio (KR) were used in this study to consider the sustainability of the current irrigation practices, and were computed using the following equations:

$$SAR = \frac{Na^+}{\sqrt{(Ca^{2+} + Mg^{2+})/2}} \quad (4)$$

$$RSC = (CO_3^- + HCO_3^-) - (Ca^{2+} + Mg^{2+}) \quad (5)$$

$$\%Na = [\frac{(Na^+ + K^+)}{(Na^+ + K^+ + Ca^{2+} + Mg^{2+})} \times 100 \quad (6)$$

$$KR = \frac{Na^+}{Ca^{2+} + Mg^{2+}} \quad (7)$$

where all the ions are expressed in milliequivalent per liter

4. Results

4.1. Hydrochemical properties from the mountain to the piedmont

The electrical conductivity (EC) is very low for mountain streamflow (average = 273 µS/cm), increases slightly for mountain springs (average = 328 µS/cm), and more substantially for piedmont groundwater (average = 807 µS/cm) (Table 2). For groundwater,

only 14 of the 55 groundwater samples exceed 1000 µS/cm, and two samples exceed 2000 µS/cm (well W17). The groundwater EC is lower in the irrigation area (mean = 727 µS/cm and max = 1094 µS/cm) than the non-irrigation area (mean = 994 and max = 2620 µS/cm). From the dry (September to November) to the wet (January to March) season the EC decreased in streamflow from 324 µS/cm to 244 µS/cm in average, and in the groundwater beneath the irrigation area from 841 µS/cm to 692 µS/cm (Table 2). The pH is higher in the mountain stream water (an average of 7.94 and a maximum of 9.1) than in piedmont groundwater (an average of 7.58 and a maximum of 8.37).

The major ion compositions are similar in streamflow and springs, but undergoes a concentration increase in the piedmont groundwater (Fig. 4, table 2), which is enriched particularly of Ca^{2+}, Mg^{2+} and HCO_3^-. The irrigation area mostly has lower major ion concentrations compared with groundwater from the non-irrigated area (Fig. 4); the largest differences are observed for Na^+ and Cl^-, whose mean values increase by 46 and 44 % respectively in the non-irrigated area.

On the Piper diagram (Fig. 5), the hydrochemical facies of the streamflow is of Ca-HCO_3 type similar to that of atmospheric precipitation (rain and snow). Compared to precipitation, a slight enrichment of Na^+, Mg^{2+} and SO_4^{-2} is observed. The majority of the groundwater in the piedmont also has a Ca-HCO_3 facies (Fig. 5). It shows in addition two secondary facies, Ca-Mg-Cl and Na-Cl related to specific enrichment in Cl^-, Na^+, and Mg^{2+}. Indeed, 7 wells located close to the Ourika wadi exhibit Ca-Mg-Cl facies. 3 wells in the non-irrigated area, W17, W19 and W27, have Na-Cl facies; they are close to a tributary, Elmaleh wadi (Elmaleh in Arabic means the salty), which drains the low-altitude halite-rich terrains.

Figure 6 shows that most of the major ions (Cl^-, HCO_3^-, Na^+, Ca^{2+}, and K^+) have decreased from the dry to wet season in terms of median, maximum and minimum. This is also reflected in the decrease of EC from the dry to wet season, and these results indicate that a dilution in the wet season has occurred following irrigation using streamflow diversion. In contrast, SO_4^{2-} and Mg^{2+} concentrations increased in terms of the median during the wet season, and NO_3^- showed a significant increase from the dry to the wet season.

4.2. Nitrates

Nitrogen is an important plant nutrient that is naturally present in the environment, but often in very low concentrations (< 10 mg/L; Hill, 1996). The multiple natural origins of nitrates are related to evaporative enrichment of dry and wet deposition, biogenic sources through bacterial activity in soil, or to a geogenic origin (Stadler et al., 2008). In the study

area, additional sources of nitrogen might also originate from fertilizers (from animal waste) or animal and domestic sewage.

The results of the nitrate ($NO^-_{3)}$ in this study show low concentrations in the streamflow (average = 3.2 mg/l, and a max of 8.2 mg/L) and springs (average = 3.8 mg/l, and a max of 7.2 mg/L), and in piedmont groundwater, the nitrate concentrations are higher (10.1 mg/l in average). Furthermore, nitrates increase slightly from the dry season (average = 8.4 mg/l) to the wet season (average = 12 mg/l). This is explained by an accumulation of NO^-_3 in the soil during the dry period and its leaching from the soil by rainfall and irrigation returns that are more important during the wet period. Despite this increase in NO^-_3 during irrigation recharge, the groundwater NO^-_3 concentrations in the irrigation area remains well below the WHO standards fixed at 50 mg/L (WHO, 2017).

4.3. Quality of drinking and irrigation water

Domestic water needs in the study area are supplied by groundwater. The small towns, that are host to tens to hundreds of inhabitants, use community-managed wells and some inhabitants still use their own wells to meet their domestic needs. Groundwater from these wells is usually used without further treatment, but occasional chlorination, which constitutes a potential health risk if the quality of this water is or becomes unsuitable for human use. Groundwater is also used for irrigation in the study area during extended dry periods. In the irrigated area, groundwater is used during summer and autumn months when streamflow is absent. In the non-irrigated area, rain-fed agriculture is dominant but some farmers use groundwater to irrigate olive fields.

The overall quality of groundwater can be assessed by the water quality index (WQI) (Talib et al., 2019, Sadat-Noori et al. 2014). WQI values are classified into five categories (calculated using the parameters …): excellent (<50), good (>50), poor (>100), very poor (>200) and water unsuitable for drinking (>300). The WQI values ranges from 3 to 95 with a mean of 24. According to this classification, almost all groundwater and surface water are "excellent" for drinking purposes. Only the 03 samples of the non-irrigated area and contaminated by salts are close to the "poor "quality category. Although groundwater is of good quality from a mineral perception, additional biological analyses are needed to fully assess the adequacy of groundwater to human use.

The suitability of groundwater for irrigation is assessed through the Wilcox diagram (Fig. 7) and various irrigation water quality indices, such as SAR, RSC, %Na and KR (Table 3). As a conclusion, most of the water is suitable for irrigation. Those few presenting unsuitable

355 characteristics due the Na^+ content correspond to the samples collected from the well W17,
356 which is characterized by high Na^+ and Cl^- concentrations and located outside of the irrigated
357 area. Compared to the others wells in the study area, the well W17 is influenced by the
358 dissolution of evaporites.

359 ## 5. Discussion

360 ### 5.1. Origins of ions in mountains water and groundwater

361 The natural chemical composition of water is potentially influenced by atmospheric
362 precipitation, evaporation, transpiration, evaporite dissolution and rock weathering. In
363 mountain waters Ca^{2+}, HCO_3^-, Na^+, Mg^{2+}, SO_4^{2-} ions are likely sourced firstly from
364 precipitation and secondly from the weathering of silicate minerals in the crystalline rocks of
365 the High-Atlas massif. The piedmont groundwater samples show similar facies with mountain
366 water, however their relatively higher concentrations of Na^+, Cl^-, and in a lesser proportion of
367 Ca^{2+}, Mg^{2+} and HCO_3^- suggest additional sources of mineralization.

368 On the Na^+/Cl^- versus Cl^- scatter diagram (Fig. 8), samples with Na/Cl ratios close to 1
369 with increasing Cl^- concentrations indicate either halite dissolution (Hao et al., 2020; Talib et
370 al., 2019), evaporation or transpiration is the major process increasing Na^+ and Cl^-
371 concentrations. The groundwater samples from the non-irrigated area exhibit little changes in
372 the Na^+/Cl^- ratio with high Cl^- concentrations (> 10 meq/L). A previous study by Bouimouass
373 et al. (2020) using the stable isotope values of groundwater for the same samples, showed no
374 evidence of evaporation effects. Therefore, high Na^+ and Cl^- concentrations in groundwater
375 are driven by either Triassic halite dissolution and/or transpiration processes. For Cl^-
376 concentrations lower than 10 meq/L, there are greater variations in the Na/Cl ratio that
377 indicates either contributions from rock weathering reactions (Na/Cl > 1) or ion exchange
378 effects (Na/Cl < 1). Based on the Na/Cl ratio, the piedmont groundwater is divided into two
379 groups (Fig. 6). The sodium enriched group n° 1 (where Na/Cl > 1), which is similar to the
380 mountain streamflow Na/Cl ratios, is mostly located in the irrigation area. The sodium
381 depleted group n° 2 (where Na/Cl < 1) is predominantly composed of samples located along
382 the Ourika wadi.

383 For group n° 1 (Na/Cl > 1) representing the irrigation area, the enrichment of Na could be
384 due to weathering by the streamflow in the mountains of the Na-silicate such as albite and
385 plagioclase (equations 8 and 9) (Gao et al., 2020) since Na-silicates are largely present in the
386 High-Atlas as granodiorite and granite.

387 $$2NaAlSi_3O_8\ (Albite) + 9H_2O + 2H_2CO_3 = Al_2Si_2O_5(OH)_4 + 2Na^+ + 2HCO_3^- + 4H_4SiO_4 \quad (8)$$

388 $(Na_{0.82}Ca_{0.18})Al_{1.18}Si_{2.82}O_8$(Plagioclase) + 1.18CO2 + 1.77H_2O = 0.82Na^+ + 0.18Ca^{2+} +

389 1.18HCO_3^- + 0.59$Al_2Si_2O_5(OH)_4$ + 1.64SiO_2 (9)

390 In the HCO_3^- versus Na^+ plot (Fig. 9a), water samples falling along the 1:1 and 1.18:0.82
391 lines indicate albite and plagioclase weathering might increase HCO_3^- and Na^+ in water (Kim
392 et al., 2002; Zhang et al., 2020). All streamflow and mountain groundwater lie along and
393 above the line 1.18:0.82 indicating contribution from weathering of albite and plagioclase to
394 Na^+ and HCO_3^- in these waters. The majority of the piedmont groundwater samples lie on or
395 between the two lines (Fig. 9a) implying that weathering of albite and plagioclase is
396 responsible for amounts of Na^+ and HCO_3^-. The groundwater samples contaminated by salts
397 plot far to the right of the 1:1 line. The additional sources of HCO_3^- ion could originate from
398 various sources including calcite dissolution (equation 10), and Ca-silicates weathering such
399 as anorthite (equation 11), pyroxene (equation 12) and amphibole (equation 13) (Zhang et al.,
400 2020). Based on chemical reactions 10, 11, 12 and 13, samples falling along the lines 1:1, 2:1,
401 1.7:1, 7:2 in figure 5b are due to the dissolution of carbonates such as calcite and dolomite,
402 and the weathering of Ca-silicates such as anorthite, pyroxene and amphibole, respectively.
403 All mountains streamflow and springs samples, and most of the piedmont groundwater
404 samples fall between the lines 1:1 and 1.7:1 (Fig. 9b) indicating that the dissolution of calcite
405 and some Ca-silicates such as pyroxene contributes to HCO_3^- concentrations in these waters.

406 $CaCO_3 + CO_2 + H_2O = Ca^{2+} + 2HCO_3^-$ (10)

407 $2CaAl_2Si_2O_8$(Anorthite) + $4CO_2 + 6H_2O = 2Al_2Si_2O_5(OH)_4 + Ca^{2+} + 4HCO_3^-$ (11)

408 $CaMg_{0.7}Fe_{0.3}Si_2O_6$(Pyroxene) + $3.4CO_2 + 2.3H_2O = Ca^{2+} + 0.7Mg^{2+} + 2SiO_2 + 3.4HCO_3^- + 0.3H^+$ +

409 $0.3Fe(OH)_3$ (12)

410 $Ca_2Mg_5Si_8O_{22}(OH)_2$(Ampibole) + $14CO_2 + 22H_2O = 2Ca^{2+} + 5Mg^{2+} + 14HCO_3^- + 8H_4SiO_4$ (13)

411 For group n° 2 (where Na/Cl < 1) representing the piedmont groundwater along the wadi,
412 the ion exchange processes and anthropogenic sources of Cl^- (Celestino et al., 2012) could be
413 responsible of Na depletion or Cl^- enrichment. The plot of Na^++K^+–Cl^- versus Ca^{2+}+Mg^{2+}–
414 SO_4- HCO_3^- (Fig. 9b) shows a linear relationship with a slope of -0.83, close to -1, indicating
415 the occurrence of ion exchange (Garçia, 2001; Yang et al., 2016). Cation exchange processes
416 were analysed using the chloro-akaline indices (CAI-I and CAI-II), which are widely used as
417 indicators of ion exchange occurring in aquifers (Schoeller, 1965; Li et al., 2013; Talib et al.,
418 2019). The indices, expressed by the equations 14 and 15, are negative when the cation
419 exchange occurs, meaning that Na^+ is released from the medium in exchange with Ca^{2+} and

Mg^{2+} in water. However, positive indices mean that Na^+ is adsorbed in the medium simultaneously with the release of Ca^{2+} and Mg^{2+}, known as reverse ion exchange.

$$\text{CAI} - \text{I} = \frac{Cl^- - (Na^+ + K^+)}{Cl^-} \quad (14)$$

$$\text{CAI} - \text{II} = \frac{Cl^- - (Na^+ + K^+)}{HCO_3^- + SO_4^{2-} + CO_3^{2-} + NO_3^-} \quad (15)$$

Piedmont groundwater samples are almost equally distributed between positive and negative CAI-1 and CAI-2 values (Fig. 9c) (25 samples with positive values, 23 with negative values and 04 with CAI-I and CAI-II equal to 0). This indicates that both base cation exchange (positive CAI-1 and CAI-2 values) and reverse ion exchange (negative CAI-1 and CAI-2) potentially occur. Along the wadi (group 2), the base cation exchange dominates implying depletion of Na^+ in groundwater. Reverse ion exchange characterizes groundwater beneath the irrigation area (Group 1), it induces a release of Na^+ of the aquifer matrix in groundwater and adsorption of Ca^{2+} and Mg^{2+} (Carol et al., 2012; Zaidi et al., 2015).

Ca^{2+} in water could also be due to gypsum dissolution, alongside SO_4^{2-}, as indicated by the equation 17. A Ca^{2+}/SO_4^{2-} ratio around 1 indicates that these ions are derived from gypsum dissolution. The majority of samples (Fig. 9f) are plot to the left of the 1:1 line indicating an excess of Ca^{2+} over SO_4^{2-} ; the Gypsum would be responsible of low amounts of Ca^{2+} and Mg^{2+}.

$$CaSO_4 \text{ (Gypsum)} = Ca^{2+} + SO_4^{2-} \quad (17)$$

5.2. Hydrochemical evolution from the mountain to the piedmont

In the high-Atlas Mountains, the streamflow and springs are supplied by rainfall and snowmelt, and flow through large outcrops of silicates rocks formed of Precambrian Granodiorite and Gneiss containing plagioclase, amphibole and micaschist, as well as Visean and Triassic siltite and sandstone rocks. They have a Ca-HCO_3 facies similar to that of atmospheric precipitation, and a slight enrichment in Na^+, Mg^{2+} and SO_4^-. In mountains streamflow and springs, Na^+ and HCO_3^- are strongly correlated ($R^2 = 0.84$, table 4), their main source is Na-silicates weathering. The Ca-silicate weathering also contributes to the loading of Ca^{2+} and Mg^{2+}. The pyroxene, amphiboles and calcic feldspar are common minerals in basic rocks and are easily weathered (Jacks 1973; Bartarya 1993; Rajmohan and Elango, 2004). Therefore, these minerals are also likely to contribute to the ionic composition of the waters in the mountains. The elevated SO_4^{2-} might also be due to the dissolution of gypsum.

In the piedmont, groundwater is generally fresh (EC average = 713 µS/cm), with a dominant Ca-HCO_3 facies similar to the streamflow. This similarity results from the recharge of the alluvial aquifer in the piedmont via irrigation of the streamflow waters, and also from in-stream losses (Bouimouass et al., 2020). Therefore, piedmont groundwater primarily inherits the hydrochemical characteristics of the high-altitude mountain water. When evolving in the piedmont and compared to streamflow, groundwater acquires a higher total mineralization and exhibits two secondary facies, Ca-Mg-Cl and Na-Cl.

The generally higher ion content of the groundwater in the piedmont compared to the recharging streamflow could be explained by transpiration processes and water-rock interactions in the alluvial aquifer. In this semi-arid study area, even though the evaporative demand is high (around 1600 mm/year), evaporation effects on piedmont groundwater were not detected from the stable isotope data presented in Bouimouass et al., (2020). This could be explained by the rapid infiltration of irrigation water, the recharge of unevaporated mountain streamflow, and by a deep unsaturated zone (4-50 m depth) that increases during the summer months (Bouimouass et al., 2020).

The secondary Na-Cl facies in piedmont groundwater was observed in the right side of the wadi in the non-irrigation area, and is either due to halite dissolution from Triassic deposits or transpiration. The Ca-Mg-Cl facies was observed near the wadi, along with the Na^+ depletion; this can be ascribed to cation exchange inducing Na^+ adsorption and, Ca^{2+} and Mg^{2+} release in groundwater. Beneath the irrigated area, reverse ion exchange was related to Na^+ enrichment; it seems that the irrigation recharge transfers Ca^{2+} and Mg^{2+} that are adsorbed by clay minerals whilst Na^+ is released in the groundwater. The occurrence of this process might be explained by the dynamics of the seasonal recharge of the diverted streamflow from the Ourika wadi. Traditional irrigation by flooding relatively large lands with streamflow induces more interaction between surface water and sediment matrix during percolation.

5.3. Effects of the traditional irrigation on the groundwater quality

In our piedmont study area, the irrigation area has the prime location of being at the foot of a major mountain range that is lowly populated and cultivated, and where streamflow is supplied by rainfall and snowmelt generally from winter to early summer. The diverted streamflow by a network of irrigation channels managed by community-driven systems is of low EC and NO_3 (273 µS/cm and 3.2 mg/L respectively), and such features constitute favorable factors of groundwater quality since the streamflow is the main groundwater recharge source. The piedmont groundwater beneath the irrigated area is characterized by

484 excellent to good chemical quality regarding both drinking and irrigation use indices. The
485 substantial induced recharge from irrigation flow leads to seasonal groundwater renewal, and
486 counterbalances effects of salinization mechanisms that often characterize irrigated arid zones
487 (Foster et al., 2018). Almost all the ions showed a dilution from the dry to the wet season. The
488 results of this study highlight a system where the irrigation practices have not adversely
489 impacted groundwater resource quality. The irrigation practices have not significantly
490 adversely altered processes controlling the major ion composition, nor are there significant
491 transfers of nitrogen-based fertilizers to the shallow groundwater. Thus, the traditional
492 irrigation practices in this mountain piedmont, which have been in place for hundreds of
493 years, are considered a low impact practice in terms of groundwater resource quality and even
494 an enhancing factor of groundwater quality.

495 More intensive and modern agricultural and irrigation practices are currently observed in
496 the neighboring plain. Within this plain, the intensive modern agriculture has had severe
497 impacts on groundwater quantity, with hydraulic heads decreasing by 1 to 3 m/year (Fakir et
498 al., 2015, Le Page et al., 2021), the groundwater nitrate concentrations are increasing
499 (Boukhari et al., 2015), and the soil salinity as well (Sefiani et al., 2019). This expansion of
500 irrigated agriculture threats the existence of the traditional agriculture system of the piedmont
501 and disturb its ecosystem. The studied traditional irrigation piedmonts, irrigated by high
502 mountain streamflow, is one of the rare sustainable human exploits that is likely to remain as
503 a low environmental impact practice. Such systems represent a strong connection and a long
504 history between water and users to ensure sustainability and drought survival, and have
505 constituted a main driver of socio-economic activities for centuries. A key success of survival
506 of such ancestral systems is the sense of mutualism between the users. This mutualism,
507 defined by Gunda et al., (2018), is the feeling of collective well-being including social
508 identity, pride of place, and maintenance of historical traditions. For those piedmonts, the
509 current traditional agricultural practices should be maintained and enhanced in order to
510 preserve their groundwater resources sustainability as they provide a nexus between food
511 production, low energy costs (streamflow diversions by gravity-fed channels), and low
512 environmental impacts. This will also benefit groundwater resources in down-gradient areas
513 since piedmonts are generally favorable recharge zones in (semi)arid basins (Wilson and
514 Guan, 2004; Liu and Yamanaka, 2012). The traditional agriculture could be improved by
515 introducing organic agriculture (FAO, 2013) that could increase the financial incomes of
516 farmers, better optimize irrigation water and increase its value.

6. Conclusion

The present study investigated the impact of groundwater recharge from a traditional irrigation system on groundwater quality in a semiarid piedmont. Groundwater hydrochemistry is controlled mainly by water-rock interactions rather than anthropogenic activities. Groundwater chemistry is influenced by both the chemical characteristics of the streamflow acquired in the mountains, and by local hydrochemical processes that occur during infiltration and recharge via the alluvial plain. Groundwater benefits from substantial seasonal recharge from diverted streamflow irrigation, which counterbalances the potential effects of salinization mechanisms common in irrigated areas of (semi)arid zones, such as evaporation and leaching of saline soils. Nitrate concentrations slightly increase with irrigation season but remain well below the permissible limits for drinking water. Almost all groundwater and surface water are "excellent" for drinking and irrigation purposes. The current state of groundwater chemistry in the piedmont of the High-Atlas is a heritage of hundreds of years of exploitation. The hydrological processes, the irrigation practices and the use by local farmers of organic fertilization have preserved the traditional hydro-agro-systems that are close to sustainable agricultural systems. Protection measures of these irrigation systems should be considered in the framework of adaptive strategies for sustainable management and for water heritage, as this system is undergoing severe pressure climate change effects and by the expansion of intensive modern agricultural practices overexploiting the water resources.

Acknowledgments

This research was funded by (a) Geosciences Semlalia laboratory of Cadi Ayyad University, (b) UMR EMMAH of Avignon University, (c) SAGESSE (program of the Moroccan ministry of higher education; Grant agreement PPR/2015/48), the FP7 International Cooperation (CHAAMS, ERANET3-062) and ASSIWAT project (UM6P, Benguerir). We would like to also thank the CNRST (Centre National pour la recherche scientifique et technique) for awarding the excellence PhD scholarship to Houssne Bouimouass.

548

549

550

551

552

553

References

554 Baba, M. W., Gascoin, S., Jarlan, L., Simonneaux, V., & Hanich, L. (2018). Variations of the
555 Snow Water Equivalent in the Ourika catchment (Morocco) over 2000–2018 using
556 downscaled MERRA-2 data. Water, 10(9), 1120.

557 Banna, M. H., Imran, S., Francisque, A., Najjaran, H., Sadiq, R., Rodriguez, M., & Hoorfar,
558 M. (2014). Online drinking water quality monitoring: review on available and emerging
559 technologies. Critical Reviews in Environmental Science and Technology, 44(12), 1370-1421.

560 Bartarya, S. K. (1993). Hydrochemistry and rock weathering in a sub-tropical Lesser
561 Himalayan river basin in Kumaun, India. Journal of Hydrology, 146, 149-174.

562 Berghuijs, W. R., Woods, R. A., & Hrachowitz, M. (2014). A precipitation shift from snow
563 towards rain leads to a decrease in streamflow. Nature Climate Change, 4(7), 583-586.

564 Boudhar, A., Hanich, L., Boulet, G., Duchemin, B., Berjamy, B., & Chehbouni, A. (2009).
565 Evaluation of the snowmelt runoff model in the Moroccan high Atlas Mountains using two
566 snow-cover estimates. Hydrological Sciences Journal, 54(6), 1094–1113.

567 Boudhar, A., Boulet, G., Hanich, L., Sicart, J. E., & Chehbouni, A. (2016). Energy fluxes and
568 melt rate of a seasonal snow cover in the Moroccan high atlas. Hydrological Sciences Journal.

569 Boukhari, K., Fakir, Y., Stigter, T. Y., Hajhouji, Y., & Boulet, G. (2015). Origin of recharge
570 and salinity and their role on management issues of a large alluvial aquifer system in the
571 semi-arid Haouz plain, Morocco. Environmental Earth Sciences, 73(10), 6195–6212.

572 Bozdağ, A. (2015). Combining AHP with GIS for assessment of irrigation water quality in
573 Çumra irrigation district (Konya), Central Anatolia, Turkey. Environmental earth
574 sciences, 73(12), 8217-8236.

575 Bresciani, E., Cranswick, R. H., Banks, E. W., Batlle-Aguilar, J., Cook, P. G., & Batelaan, O.
576 (2018). Using hydraulic head, chloride and electrical conductivity data to distinguish between
577 mountain-front and mountain-block recharge to basin aquifers. Hydrology and Earth System
578 Sciences, 22(2), 1629-1648.

579 Buschmann, J., Berg, M., Stengel, C., Winkel, L., Sampson, M. L., Trang, P. T. K., & Viet, P.
580 H. (2008). Contamination of drinking water resources in the Mekong delta floodplains:

582 Arsenic and other trace metals pose serious health risks to population. Environment
583 international, 34(6), 756-764.

584 Carol, E. S., Kruse, E. E., Laurencena, P. C., Rojo, A., & Deluchi, M. H. (2012). Ionic
585 exchange in groundwater hydrochemical evolution. Study case: the drainage basin of El
586 Pescado creek (Buenos Aires province, Argentina). Environmental Earth Sciences, 65(2),
587 421-428.

588 Cartwright, I., Hannam, K., & Weaver, T. R. (2007). Constraining flow paths of saline
589 groundwater at basin margins using hydrochemistry and environmental isotopes: Lake
590 Cooper, Murray Basin, Australia. Australian Journal of Earth Sciences, 54(8), 1103-1122.

591 Celestino, A. E. M., Leal, J. A. R., Cruz, D. A. M., Vargas, J. T., JOSUE, D. L. B., &
592 Ramírez, J. M. (2019). Identification of the hydrogeochemical processes and assessment of
593 groundwater quality, using multivariate statistical approaches and water quality index in a
594 wastewater irrigated region.

595 Chen, J., He, D., & Cui, S. (2003). The response of river water quality and quantity to the
596 development of irrigated agriculture in the last 4 decades in the Yellow River Basin,
597 China. Water Resources Research, 39(3).

598 Coyte, R. M., Singh, A., Furst, K. E., Mitch, W. A., & Vengosh, A. (2019). Co-occurrence of
599 geogenic and anthropogenic contaminants in groundwater from Rajasthan, India. Science of
600 the Total Environment, 688, 1216-1227.

601 Delcaillau, B., Amrhar, M., Namous, M., Laville, E., Pedoja, K., & Dugué, O. (2011).
602 Transpressional tectonics in the Marrakech High Atlas: insight by the geomorphic evolution
603 of drainage basins. Geomorphology, 134(3-4), 344-362.

604 Duncan, R. A., Bethune, M. G., Thayalakumaran, T., Christen, E. W., & McMahon, T. A.
605 (2008). Management of salt mobilisation in the irrigated landscape–A review of selected
606 irrigation regions. Journal of Hydrology, 351(1-2), 238-252.

607 Druhan, J. L., Hogan, J. F., Eastoe, C. J., Hibbs, B. J., & Hutchison, W. R. (2008).
608 Hydrogeologic controls on groundwater recharge and salinization: a geochemical analysis of
609 the northern Hueco Bolson aquifer, Texas, USA. Hydrogeology Journal, 16(2), 281-296.

610 Elmeknassi, M., El Mandour, A., Elgettafi, M., Himi, M., Tijani, R., El Khantouri, F. A., &
611 Casas, A. (2021). A GIS-based approach for geospatial modeling of groundwater
612 vulnerability and pollution risk mapping in Bou-Areg and Gareb aquifers, northeastern
613 Morocco. Environmental Science and Pollution Research, 1-20.

614 Exner, M. E., Hirsh, A. J., & Spalding, R. F. (2014). Nebraska's groundwater legacy: Nitrate
615 contamination beneath irrigated cropland. Water Resources Research, 50(5), 4474-4489.

616 Fakir Y., Berjamy B., Le Page M., Sghrer F., Nasah H., Jarlan L., Er Raki S., Simonneaux V.,
617 Khabba S. (2015). Multi-modeling assessment of recent changes in groundwater resource:
618 Application to the semi-arid Haouz plain (Central Morocco). EGU General Assembly, Vol.
619 17, EGU2015-14624.

620 FAO. 2013. Organic supply chains for small farmer income generation in developing
621 countries – Case studies in India, Thailand, Brazil, Hungary and Africa. Rome.

FAO, IWMI, 2018.More People, More Food, Worse Water? A Global Review of Water Pollution from Agriculture. Food and Agriculture Organization of the United Nations andInternational Water Management Institute (224 pp).

Fernald, A., Guldan, S., Boykin, K., Cibils, A., Gonzales, M., Hurd, B., … Rodriguez, S. (2015). Linked hydrologic and social systems that support resilience of traditional irrigation communities. Hydrology and Earth System Sciences, 19(1), 293–307.

Foster, S. S. D., & Chilton, P. J. (2003). Groundwater: the processes and global significance of aquifer degradation. Philosophical Transactions of the Royal Society of London. Series B: Biological Sciences, 358(1440), 1957-1972.

Foster, S. S. D., & Perry, C. J. (2010). Improving groundwater resource accounting in irrigated areas: a prerequisite for promoting sustainable use. Hydrogeology Journal, 18(2), 291-294.

Foster, S., Pulido-Bosch, A., Vallejos, Á., Molina, L., Llop, A., & MacDonald, A. M. (2018). Impact of irrigated agriculture on groundwater-recharge salinity: a major sustainability concern in semi-arid regions. Hydrogeology Journal, 26(8), 2781-2791.

Gao, J., Zou, C., Li, W., Ni, Y., Liao, F., Yao, L., ... & Vengosh, A. (2020). Hydrochemistry of flowback water from Changning shale gas field and associated shallow groundwater in Southern Sichuan Basin, China: Implications for the possible impact of shale gas development on groundwater quality. Science of The Total Environment, 713, 136591.

Gunda, T., Turner, B. L., & Tidwell, V. C. (2018). The influential role of sociocultural feedbacks on community-managed irrigation system behaviors during times of water stress. Water Resources Research, 54(4), 2697-2714.

Hajhouji, Y., Simonneaux, V., Gascoin, S., Fakir, Y., Richard, B., Chehbouni, A., & Boudhar, A. (2018). Modélisation pluie-débit et analyse du régime d'un bassin versant semi-aride sous influence nivale. Cas du bassin versant du Rheraya (Haut Atlas, Maroc). La Houille Blanche, 3 (2018), 49–62.

Hajhouji Y., Fakir Y., Simonneaux V., Gascoin S., Bouras E.H., Chehbouni A. (2020) Effects of Climate Change at the 2040's Horizon on the Hydrology of the Pluvio-Nival Rheraya Watershed Near Marrakesh*, Morocco. In: El Moussati A., Kpalma K., Ghaouth Belkasmi M., Saber M., Guégan S. (eds) Advances in Smart Technologies Applications and Case Studies. SmartICT 2019. Lecture Notes in Electrical Engineering, vol 684. Springer, Cham. https://doi.org/10.1007/978-3-030-53187-4_48

Haj-Amor, Z., Tóth, T., Ibrahimi, M. K., & Bouri, S. (2017). Effects of excessive irrigation of date palm on soil salinization, shallow groundwater properties, and water use in a Saharan oasis. Environmental Earth Sciences, 76(17), 590.

Hao, Q., Xiao, Y., Chen, K., Zhu, Y., & Li, J. (2020). Comprehensive understanding of groundwater geochemistry and suitability for sustainable drinking purposes in confined aquifers of the wuyi region, Central North China plain. Water, 12(11), 3052.

Hill, M. J. (1996). Nitrates and nitrites in food and water (Vol. 7). CRC Press.

Hock, R., Rasul, G., Adler, C., Cáceres, B., Gruber, S., Hirabayashi, Y., ... & Zhang, Y. (2019). High Mountain Areas: In: IPCC Special Report on the Ocean and Cryosphere in a Changing Climate.

Hu, Q., Yang, Y., Han, S., & Wang, J. (2019). Degradation of agricultural drainage water quantity and quality due to farmland expansion and water-saving operations in arid basins. Agricultural Water Management, 213, 185-192.

Immerzeel, W. W., Van Beek, L. P., & Bierkens, M. F. (2010). Climate change will affect the Asian water towers. Science, 328(5984), 1382-1385.

Immerzeel, W. W., Lutz, A. F., Andrade, M., Bahl, A., Biemans, H., Bolch, T., ... & Emmer, A. (2020). Importance and vulnerability of the world's water towers. Nature, 577(7790), 364-369.

Jacks, G. (1973). Chemistry of ground water in a district in Southern India. Journal of Hydrology, 18(3-4), 185-200.

Jarlan, L., Khabba, S., Szcypta C., Lili-Chabaane Z., Driouech M., Le Page, M.; Hanich, L., Fakir, Y., BOONE A., Boulet G. (2016). Water resources in South Mediterranean catchments, Assessing climatic drivers and impacts. The Mediterranean Region under Climate Change, IRD ÉDITIONS, Sub-chapter 2.3.2, p: 303-308. ISBN : 978-2-7099-2219-7

Jia, H., Qian, H., Zheng, L., Feng, W., Wang, H., & Gao, Y. (2020). Alterations to groundwater chemistry due to modern water transfer for irrigation over decades. Science of The Total Environment, 717, 137170.

Jiménez-Martínez, J., Skaggs, T. H., Van Genuchten, M. T., & Candela, L. (2009). A root zone modelling approach to estimating groundwater recharge from irrigated areas. Journal of Hydrology, 367(1-2), 138-149.

Johansson, O., Aimbetov, I., & Jarsjö, J. (2009). Variation of groundwater salinity in the partially irrigated Amudarya River delta, Uzbekistan. Journal of Marine Systems, 76(3), 287-295.

Juery, A. (1976). Datation uranium-plomb du socle précambrien du Haut Atlas (Maroc). These Univ.

Juntakut, P., Snow, D. D., Haacker, E. M., & Ray, C. (2019). The long term effect of agricultural, vadose zone and climatic factors on nitrate contamination in Nebraska's groundwater system. Journal of contaminant hydrology, 220, 33-48.

Kelly, W. Use of saline irrigation water. Soil Sci. 1963, 95, 355–391

Kim, K. (2002). Plagioclase weathering in the groundwater system of a sandy, silicate aquifer. *Hydrological processes*, *16*(9), 1793-1806.

Le Page, M., Fakir, Y., Jarlan, L., Boone, A., Berjamy, B., Khabba, S., & Zribi, M. (2021). Projection of irrigation water demand based on the simulation of synthetic crop coefficients and climate change. Hydrology and Earth System Sciences, 25(2), 637-651.

Li, P., Wu, J., & Qian, H. (2013). Assessment of groundwater quality for irrigation purposes and identification of hydrogeochemical evolution mechanisms in Pengyang County, China. Environmental Earth Sciences, 69(7), 2211-2225.

Li, P., Wu, J., & Qian, H. (2016). Hydrochemical appraisal of groundwater quality for drinking and irrigation purposes and the major influencing factors: a case study in and around Hua County, China. Arabian Journal of Geosciences, 9(1), 15.

Liu, Y., & Yamanaka, T. (2012). Tracing groundwater recharge sources in a mountain–plain transitional area using stable isotopes and hydrochemistry. Journal of Hydrology, 464, 116–126.

Liu, F., Zhao, Z., Yang, L., Ma, Y., Li, B., Gong, L., & Liu, H. (2020). Phreatic Water Quality Assessment and Associated Hydrogeochemical Processes in an Irrigated Region Along the Upper Yellow River, Northwestern China. Water, 12(2), 463.

Malek, K., Reed, P., Adam, J., Karimi, T., & Brady, M. (2020). Water rights shape crop yield and revenue volatility tradeoffs for adaptation in snow dependent systems. Nature communications, 11(1), 1-10.

Marchane, A., Jarlan, L., Hanich, L., Boudhar, A., Gascoin, S., Tavernier, A., … Berjamy, B. (2015). Assessment of daily MODIS snow cover products to monitor snow cover dynamics over the Moroccan atlas mountain range. Remote Sensing of Environment, 160, 72–86.

Merchán, D., Causapé, J., Abrahão, R., & García-Garizábal, I. (2015). Assessment of a newly implemented irrigated area (Lerma Basin, Spain) over a 10-year period. II: Salts and nitrate exported. Agricultural Water Management, 158, 288-296.

Merchán, D., Sanz, L., Alfaro, A., Pérez, I., Goñi, M., Solsona, F., ... & Casalí, J. (2020). Irrigation implementation promotes increases in salinity and nitrate concentration in the lower reaches of the Cidacos River (Navarre, Spain). Science of The Total Environment, 706, 135701.

Mvandaba, V., Hughes, D., Kapangaziwiri, E., Kahinda, J. M., Hobbs, P., Madonsela, S., & Oosthuizen, N. (2018). The delineation of alluvial aquifers towards a better understanding of channel transmission losses in the Limpopo River Basin. Physics and Chemistry of the Earth, Parts A/B/C, 108, 60-73.

Nakagawa, K., Amano, H., Persson, M., & Berndtsson, R. (2021). Spatiotemporal variation of nitrate concentrations in soil and groundwater of an intensely polluted agricultural area. Scientific reports, 11(1), 1-13.

Ouanaimi, H. (2011). Haut Atlas De Marrakech, Circuit Gueliz-Ourika. Notes Mém Serv Géol Maroc, 557, 91-108.

Panda, B. R., Chidambaram, S., Ganesh, N., Adithya, V. S., Prasanna, M. V., Pradeep, K., & Vasudevan, U. (2018). A hydrochemical approach to estimate mountain front recharge in an aquifer system in Tamilnadu, India. Acta Geochimica, 37(3), 465-488.

Rabemanana, V., Violette, S., De Marsily, G., Robain, H., Deffontaines, B., Andrieux, P., ... & Parriaux, A. (2005). Origin of the high variability of water mineral content in the bedrock aquifers of Southern Madagascar. Journal of Hydrology, 310(1-4), 143-156.

738 Rajmohan, N., & Elango, L. (2004). Identification and evolution of hydrogeochemical
739 processes in the groundwater environment in an area of the Palar and Cheyyar River Basins,
740 Southern India. Environmental Geology, 46(1), 47-61.

741 Rajmohan, N. (2021). Application of water quality index and chemometric methods on
742 contamination assessment in the shallow aquifer, Ganges River basin, India. Environmental
743 Science and Pollution Research, 28(18), 23243-23257.

744 Ravindra, K., & Garg, V. K. (2007). Hydro-chemical survey of groundwater of Hisar city and
745 assessment of defluoridation methods used in India. Environmental monitoring and
746 assessment, 132(1), 33-43.

747 Rotiroti, M., Bonomi, T., Sacchi, E., McArthur, J. M., Stefania, G. A., Zanotti, C., …
748 Fumagalli, L. (2019). The effects of irrigation on groundwater quality and quantity in a
749 human-modified hydro-system: The Oglio River basin, Po plain, northern Italy. Science of the
750 Total Environment, 672, 342–356.

751 Sadat-Noori, S.; Ebrahimi, K.; Liaghat, A. Groundwater quality assessment using the Water
752 Quality Index and GIS in Saveh-Nobaran aquifer, Iran. Environ. Earth Sci. 2014, 71, 3827–
753 3843.

754 Scanlon, B. R., Jolly, I., Sophocleous, M., & Zhang, L. (2007). Global impacts of conversions
755 from natural to agricultural ecosystems on water resources: Quantity versus quality. Water
756 resources research, 43(3).

757 Schoeller, H. Qualitative Evaluation of Groundwater Resources. Methods and Techniques of
758 Groundwater Investigations and Development; UNESCO: Paris, France, 1965; Volume 5483.

759 Sefiani, S., El Mandour, A., Laftouhi, N., Khalil, N., Chehbouni, A., Jarlan, L., ... & Nassah,
760 H. (2019). Evaluation of Groundwater Quality and Agricultural use Under a Semi-arid
761 Environment: Case of Agafay, Western Haouz, Morocco. Irrigation and Drainage, 68(4), 778-
762 796.

763 Simoes, F., Moreira, A. B., Bisinoti, M. C., Gimenez, S. M. N., & Yabe, M. J. S. (2008).
764 Water quality index as a simple indicator of aquaculture effects on aquatic bodies. Ecological
765 indicators, 8(5), 476-484.

766 Sinan, M., 1986. Paramètres hydrogéologiques et géoélectriques en milieu alluvial fortement
767 hétérogène : relations statistiques et approche géostatistique comparative (exemple de la
768 nappe du Haouz-Maroc). Thèse de 3e cycle, Université Montpellier II, France, 397 p.

769 Sinan, M., 2000. Méthodologie d'identification, d'évaluation et de protection des ressources
770 en eau des aquifères régionaux par la combinaison des SIG, de la géophysique et de la
771 géostatistique. Application à l'aquifère de Haouz de Marrakech (Maroc). Thèse de Doctorat
772 d'État, Université Mohammed V, École Mohammadia d'Ingénieurs, Rabat, Maroc, 372 p.

773 Sinan, M., & Razack, M. (2006). Estimation of the transmissivity field of a heterogeneous
774 alluvial aquifer using transverse resistance. Application to the Haouz groundwater
775 (Morocco). J. Water Sci, 19(3), 221-232.

776 Stadler, S., Osenbrück, K., Knöller, K., Suckow, A., Sültenfuß, J., Oster, H., ... & Hötzl, H.
777 (2008). Understanding the origin and fate of nitrate in groundwater of semi-arid
778 environments. Journal of Arid Environments, 72(10), 1830-1842.

779 Stigter, T. Y., Dill, A. C., Ribeiro, L., & Reis, E. (2006). Impact of the shift from groundwater
780 to surface water irrigation on aquifer dynamics and hydrochemistry in a semi-arid region in
781 the south of Portugal. Agricultural water management, 85(1-2), 121-132.

782 Sun, Z., Ma, R., Wang, Y., Hu, Y., & Sun, L. (2016). Hydrogeological and hydrogeochemical
783 control of groundwater salinity in an arid inland basin: Dunhuang Basin, northwestern
784 China. Hydrological Processes, 30(12), 1884-1902.

785 Talib, M. A., Tang, Z., Shahab, A., Siddique, J., Faheem, M., & Fatima, M. (2019).
786 Hydrogeochemical characterization and suitability assessment of groundwater: A case study
787 in Central Sindh, Pakistan. International journal of environmental research and public
788 health, 16(5), 886.

789 Teng, Y., Zuo, R., Xiong, Y., Wu, J., Zhai, Y., & Su, J. (2019). Risk assessment framework
790 for nitrate contamination in groundwater for regional management. Science of the Total
791 Environment, 697, 134102.

792 Thorslund, J., & van Vliet, M. T. (2020). a global dataset of surface water and groundwater
793 salinity measurements from 1980–2019. Scientific Data, 7(1), 1-11.

794 Turner, B. L., Tidwell, V., Fernald, A., Rivera, J. A., Rodriguez, S., Guldan, S., ... & Cibils,
795 A. (2016). Modeling acequia irrigation systems using system dynamics: Model development,
796 evaluation, and sensitivity analyses to investigate effects of socio-economic and biophysical
797 feedbacks. Sustainability, 8(10), 1019.

798 Tweed, S., Celle-Jeanton, H., Cabot, L., Huneau, F., De Montety, V., Nicolau, N., ... &
799 Leblanc, M. (2018). Impact of irrigated agriculture on groundwater resources in a temperate
800 humid region. Science of the Total Environment, 613, 1302-1316.

801 Vaiphei, S. P., & Kurakalva, R. M. (2021). Hydrochemical characteristics and nitrate health
802 risk assessment of groundwater through seasonal variations from an intensive agricultural
803 region of upper Krishna River basin, Telangana, India. Ecotoxicology and Environmental
804 Safety, 213, 112073.

805 Van Steenbergen, F., Haile, A. M., Alemehayu, T., Alamirew, T., & Geleta, Y. (2011). Status
806 and potential of spate irrigation in Ethiopia. Water Resources Management, 25(7), 1899–
807 1913. DOI: 10.1007/s11269-011-9780-7

808 Vincy, M.; Brilliant, R.; Pradeepkumar, A. Hydrochemical characterization and quality
809 assessment of groundwater for drinking and irrigation purposes: A case study of Meenachil
810 River Basin, Western Ghats, Kerala, India. Environ. Monit. Assess. 2015, 187, 4217.

811 Viviroli, D., Dürr, H. H., Messerli, B., Meybeck, M., & Weingartner, R. (2007). Mountains of
812 the world, water towers for humanity: Typology, mapping, and global significance. Water
813 resources research, 43(7).

814 Viviroli, D., Archer, D. R., Buytaert, W., Fowler, H. J., Greenwood, G. B., Hamlet, A. F., ...
815 & Lorentz, S. (2011). Climate change and mountain water resources: overview and

recommendations for research, management and policy. Hydrology and Earth System Sciences, 15(2), 471-504.

Viviroli, D., Kummu, M., Meybeck, M., Kallio, M., & Wada, Y. (2020). Increasing dependence of lowland populations on mountain water resources. Nature Sustainability, 3(11), 917-928.

World Health Organization (WHO) (2011) Guidelines for drinking water quality, 4th edn. World Health Organization, Geneva, 978-92-4-154815-1

WHO (2017) Guidelines for drinking water quality: fourth edition incorporating the first addendum. World Health Organization, Geneva.

Wilson, J. L., & Guan, H. (2004). Mountain-block hydrology and mountain-front recharge. Groundwater recharge in a desert environment: The Southwestern United States, 9.

Wu, J., & Sun, Z. (2016). Evaluation of shallow groundwater contamination and associated human health risk in an alluvial plain impacted by agricultural and industrial activities, mid-west China. Exposure and Health, 8(3), 311-329.

Yang, Q., Wang, L., Ma, H., Yu, K., & Martín, J. D. (2016). Hydrochemical characterization and pollution sources identification of groundwater in Salawusu aquifer system of Ordos Basin, China. Environmental Pollution, 216, 340-349.

Xiao, Y., Gu, X., Yin, S., Pan, X., Shao, J., & Cui, Y. (2017). Investigation of geochemical characteristics and controlling processes of groundwater in a typical long-term reclaimed water use area. Water, 9(10), 800.

Xiao, J., Wang, L., Deng, L., & Jin, Z. (2019). Characteristics, sources, water quality and health risk assessment of trace elements in river water and well water in the Chinese Loess Plateau. Science of the Total Environment, 650, 2004-2012.

Xiao, Y., Yin, S., Hao, Q., Gu, X., Pei, Q., & Zhang, Y. (2020). Hydrogeochemical appraisal of groundwater quality and health risk in a near-suburb area of North China. Journal of Water Supply: Research and Technology-Aqua, 69(1), 55-69.

Xiao, Y., Hao, Q., Zhang, Y., Zhu, Y., Yin, S., Qin, L., & Li, X. (2022). Investigating sources, driving forces and potential health risks of nitrate and fluoride in groundwater of a typical alluvial fan plain. Science of The Total Environment, 802, 149909.

Nakagawa, P., Feng, W., Qian, H., & Zhang, Q. (2019). Hydrogeochemical characterization and irrigation quality assessment of shallow groundwater in the Central-Western Guanzhong Basin, China. International journal of environmental research and public health, 16(9), 1492.

Zaidi, F. K., Nazzal, Y., Jafri, M. K., Naeem, M., & Ahmed, I. (2015). Reverse ion exchange as a major process controlling the groundwater chemistry in an arid environment: a case study from northwestern Saudi Arabia. Environmental Monitoring and Assessment, 187(10), 607.

Zhang, B., Song, X., Zhang, Y., Han, D., Tang, C., Yu, Y., & Ma, Y. (2012). Hydrochemical characteristics and water quality assessment of surface water and groundwater in Songnen plain, Northeast China. Water research, 46(8), 2737-2748.

Zhang, Q., Xu, P., & Qian, H. (2020). Groundwater quality assessment using improved water quality index (WQI) and human health risk (HHR) evaluation in a semi-arid region of northwest China. Exposure and health, 1-14.

Tables

Table 1: WQI index.

Parameter	S_i (mg/l)	Weight	Relative weight
TDS	1000	5	0.13
Cl^-	250	5	0.13
SO_4^{2-}	250	5	0.13
F^-	1	5	0.13
NO^-_3	50	5	0.13
Na^+	200	4	0.10
Mg^{2+}	150	3	0.08
Ca^{2+}	200	3	0.08
K^+	12	2	0.05
HCO_3^-	250	1	0.03
		$\sum W_i = 38$	$\sum W_i = 1$

Table 2: Statistics of the field parameters and major ions.

Hydrochemical variables (mg/l)	Mountain streamflow ST (n=11)			Mountain springs SP (n=14)			Groundwater irrigation area (n=39)			Groundwater non-irrigation area (n=16)			WHO (2017)
	Min	Max	Mean	Min	Max	Mean	Min	Max	Mean	Min	Max	Mean	
pH	6.64	9.05	7.94	7	9.1	7.72	7.00	8.2	7.5	7.0	8.4	7.8	6.5-8.5
EC	104.0	563.0	273.1	77.0	943.0	328.2	293.0	1945.0	726.7	258.0	2620.0	994	
TDS	79.0	423.0	194.5	54.0	705.0	241.3	216.0	1130.0	491.2	198.0	1615.0	655.3	500
Na^+	3.3	24.7	11.7	2.6	55.4	15.39	18.1	257.7	53.6	10.2	425.5	100.0	200
K^+	0.5	2.1	1.2	0.3	3.6	1.42	0.6	1.4	3.0	0.2	2.9	1.1	200
Mg^{2+}	3.0	9.5	7.2	1.9	21.5	7.5	6.6	16.6	30.5	7.8	46.9	25.4	NA
Ca^{2+}	11.5	69.7	29.5	7.4	38.4	21.49	30.5	129. 9	64.4	27.0	111.4	59.3	200
Cl^-	3.2	32.2	14.8	2.4	79.9	19.53	17.4	462.8	93.4	7.8	719.3	167.4	250
$SO4^-_2$	6.9	27.1	16.3	5.6	70.4	23.03	11.0	91.5	29.1	2.5	149.8	39.9	200
HCO^-_3	49	256.0	110.5	27.0	371.0	132	112.2	370.9	222.8	131.8	398.9	247.3	NA
$NO3^-$	0.5	8.1	3.2	1.9	7.1	3.8	1.2	22.5	10.1	2.4	22.1	10.1	50

Table 3: Statistics of the irrigation water quality indices in the study area.

Indices	Groundwater			Surface water			Permissible limit	Unsuitable samples
	Min	Max	Mean	Min	Max	Mean		
SAR	0.2	13.4	1.6	0.2	0.8	0.5	≤ 18	-
RSC	-4.0	1.1	-0.8	-0.5	-0.1	-0.3	≤ 2.5	-
%Na	12	83	30	14.3	27.5	19.6	≤ 60	3
KR	0.1	4.9	0.5	0.1	0.3	0.2	≤ 1	3

961

962

963

964

965

966

967

968

969

970

971 *Table 4: Linear relationship (R2) between various parameters of groundwater in the study area.*

	pH	EC	TDS	Na	K	Mg	Ca	Cl	SO4	HCO3	NO3
pH	1										
EC	-0,32	1									
TDS	-0,34	0,99	1								
Na	-0,25	0,96	0,93	1							
K	-0,2	0,53	0,52	0,46	1						
Mg	-0,18	0,51	0,59	0,34	0,05	1					
Ca	-0,47	0,49	0,54	0,25	0,54	0,41	1				
Cl	-0,29	0,97	0,94	0,98	0,52	0,35	0,39	1			
SO4	0,05	0,7	0,7	0,63	0,57	0,5	0,38	0,64	1		
HCO3	-0,38	0,39	0,5	0,21	0,12	0,77	0,57	0,19	0,19	1	
NO3	0,26	-0,11	-0,05	-0,2	-0,26	0,47	-0,02	-0,22	0,02	0,28	1

972

973

Figure 1: Map of the study area and sampling points. (a) Morocco, (b) Tensift basin, and (c) sampling points in the Ourika watershed, the wadi gauging station and some principal irrigations channels (Seguias).

Figure 2: Pictures from the study area. A: a panoramic view of the agricultural crops over the piedmont, B: a Seguia diverting water directly from the Ourika stream, C, D and E: different types of Seguias in the piedmont.

Figure 3: Geology and cross section of Ourika watershed.

Figure 4: Boxplots of the major ions in groundwater (GW), spring (SP) and surface water (SW).

Figure 5: Piper diagram. Pink color refers to dry season and blue color refers to wet season.

Figure 6: Seasonal variation in EC and major ions concentrations.

Figure 7: Wilcox diagram. Red color refers to dry season and blue color refers to wet season.

Figure 8: Plot of Na/Cl ratio versus Cl. Red color refers to dry season and blue color refers to wet season.

Figure 9: Scatter plots of ions. Red color refers to dry season and blue color refers to wet season.

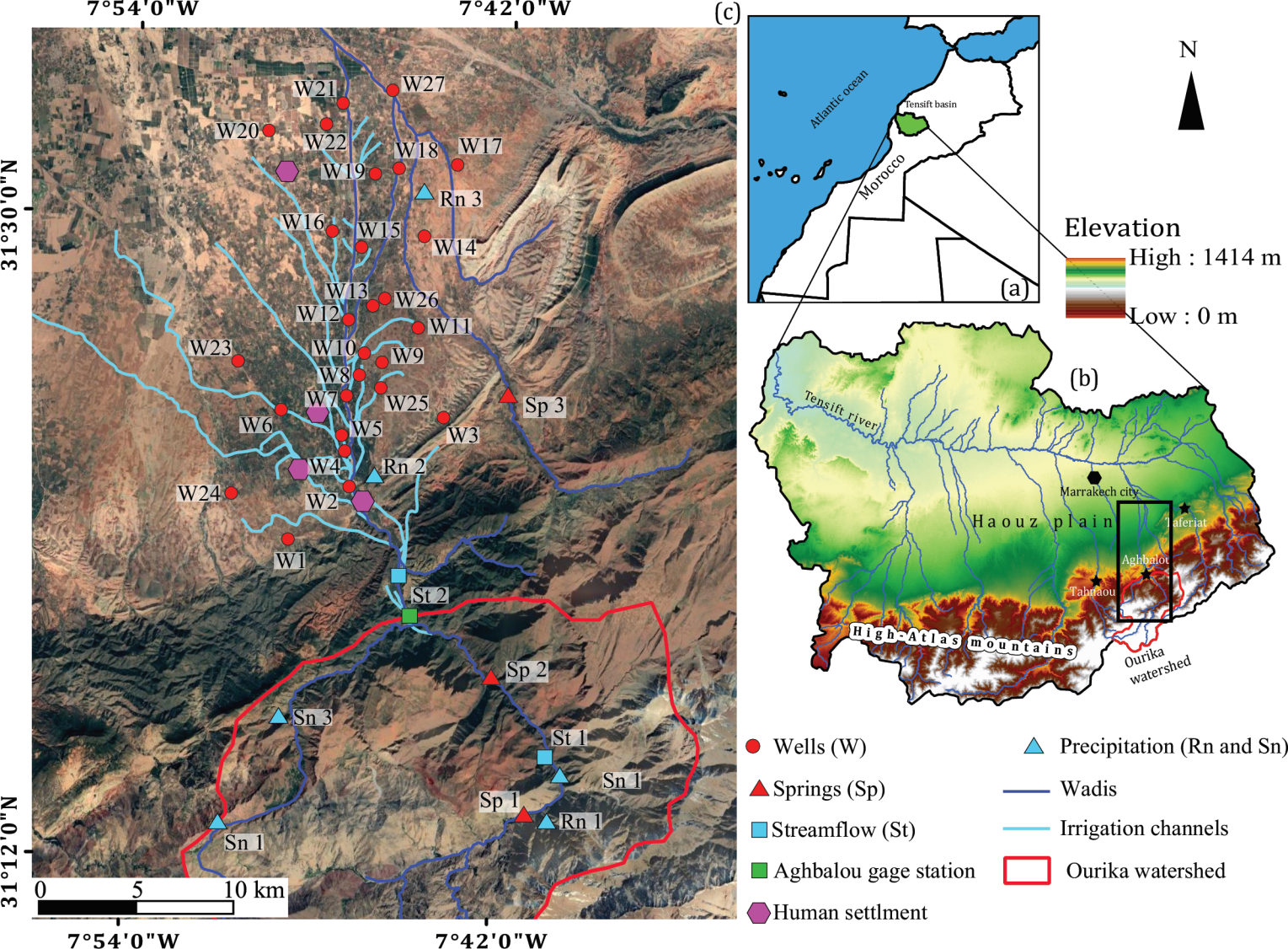
7°54'0"W
7°42'0"W
31°30'0"N
31°12'0"N
(c)
W21
W27
W20
W22
W18
W17
W19
Rn 3
W16
W15
W14
W13
W26
W12
W11
W23
W10
W9
W8
W7
W25
Sp 3
W6
W5
W3
W4
Rn 2
W24
W2
W1
St 2
Sp 2
Sn 3
St 1
Sn 1
Sp 1
Rn 1
Sn 1
0
5
10 km
Atlantic ocean
Tensift basin
Morocco
(a)
N
Elevation
High : 1414 m
Low : 0 m
(b)
Tensift river
Marrakech city
Haouz plain
Taferiat
Aghbalou
Tahnaou
High-Atlas mountains
Ourika watershed
Wells (W)
Springs (Sp)
Streamflow (St)
Aghbalou gage station
Human settlment
Precipitation (Rn and Sn)
Wadis
Irrigation channels
Ourika watershed


A
B
Stream
1st order Seguia
C
2nd order Seguia
1st order Seguia
D
3rd order Seguia

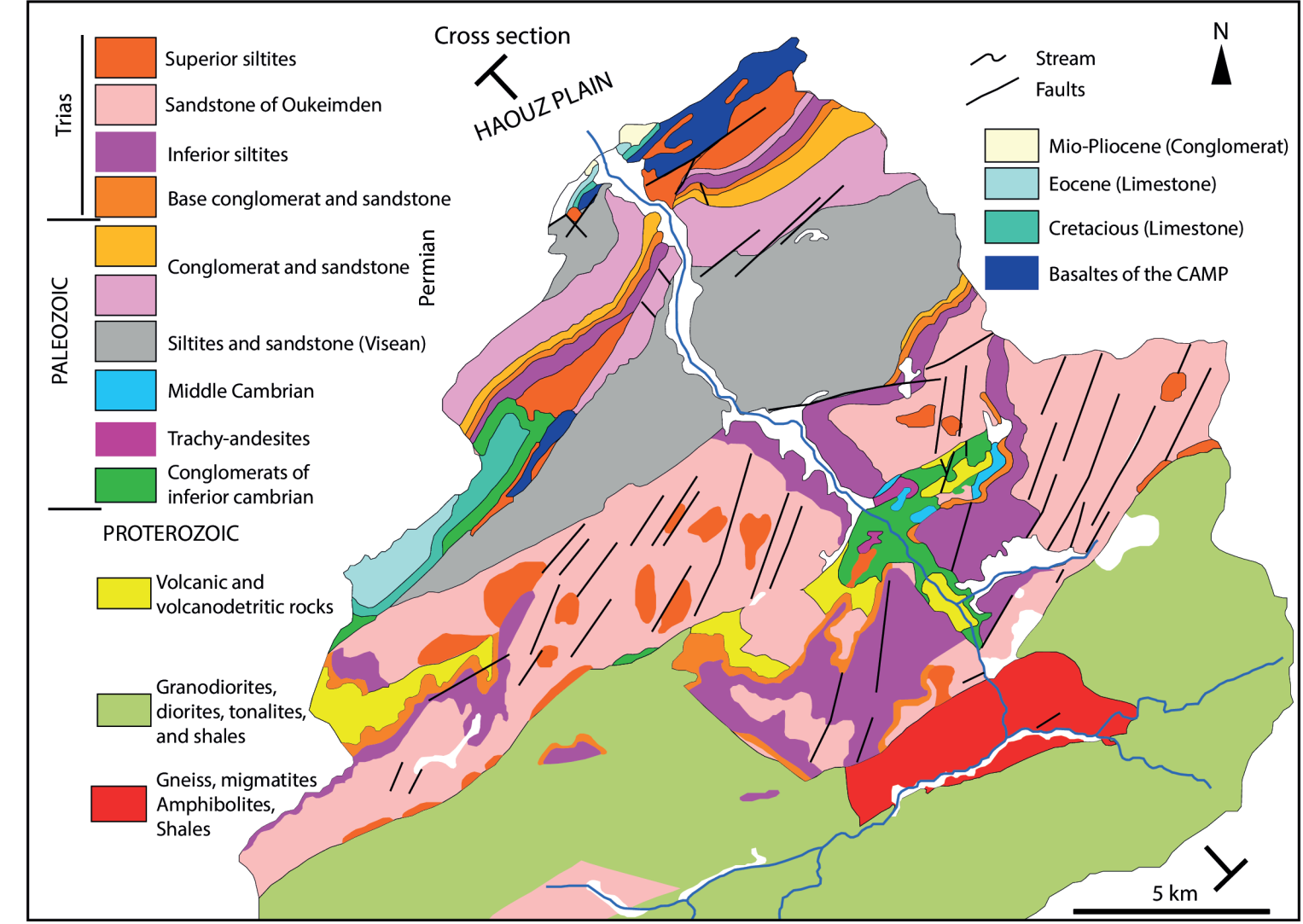
Cross section
HAOUZ PLAIN
N
Stream
Faults
Trias
Superior siltites
Sandstone of Oukeimden
Inferior siltites
Base conglomerat and sandstone
Permian
Conglomerat and sandstone
PALEOZOIC
Siltites and sandstone (Visean)
Middle Cambrian
Trachy-andesites
Conglomerats of inferior cambrian
PROTEROZOIC
Volcanic and volcanodetritic rocks
Granodiorites, diorites, tonalites, and shales
Gneiss, migmatites Amphibolites, Shales
Mio-Pliocene (Conglomerat)
Eocene (Limestone)
Cretacious (Limestone)
Basaltes of the CAMP
5 km

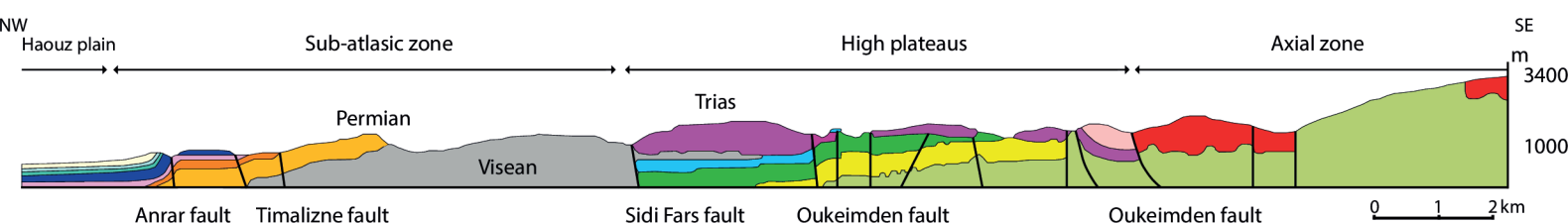
NW
SE
Haouz plain
Sub-atlasic zone
High plateaus
Axial zone
m
3400
1000
Permian
Trias
Visean
Anrar fault
Timalizne fault
Sidi Fars fault
Oukeimden fault
Oukeimden fault
0 1 2km

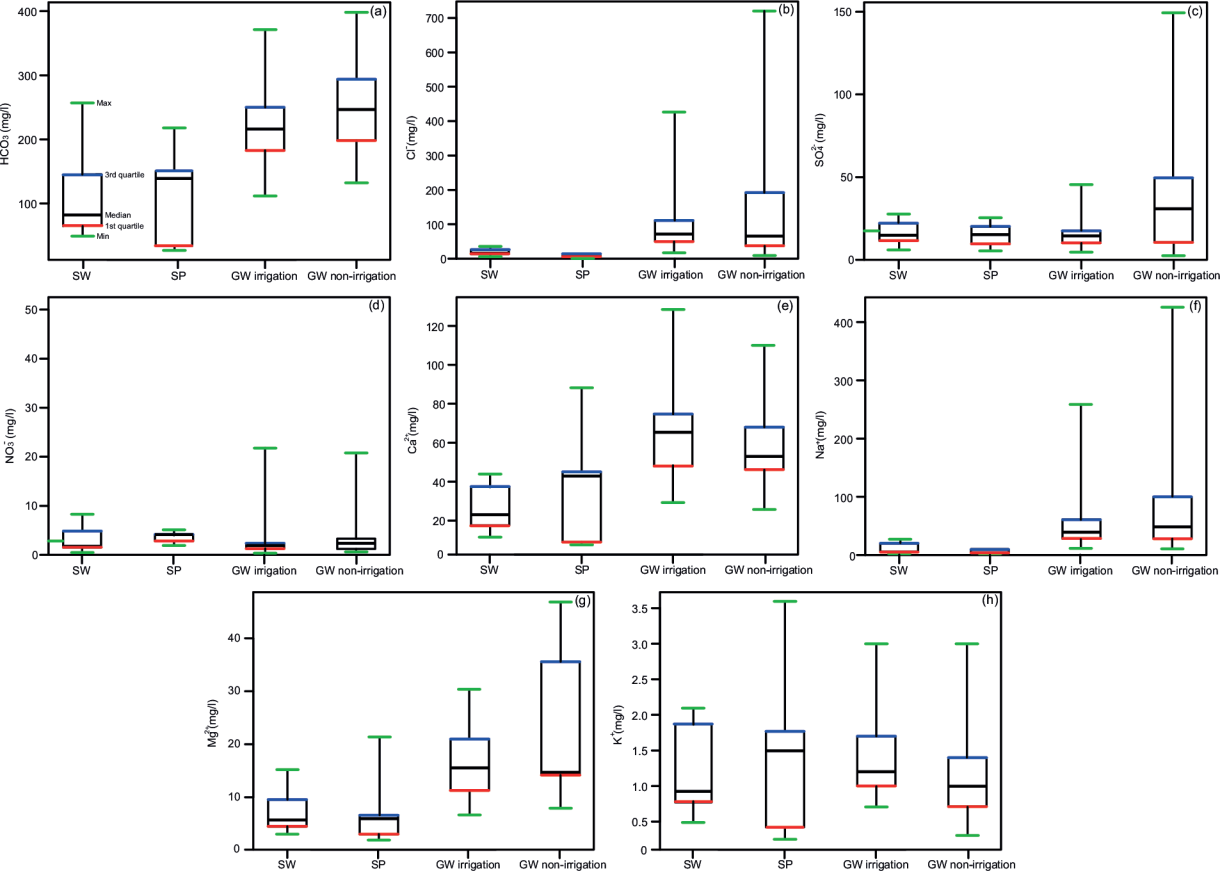
(a)
HCO3 (mg/l)
Max
3rd quartile
Median
1st quartile
Min
SW
SP
GW irrigation
GW non-irrigation
(b)
Cl (mg/l)
(c)
SO4 (mg/l)
(d)
NO3 (mg/l)
(e)
Ca2 (mg/l)
(f)
Na (mg/l)
(g)
Mg2 (mg/l)
(h)
K (mg/l)

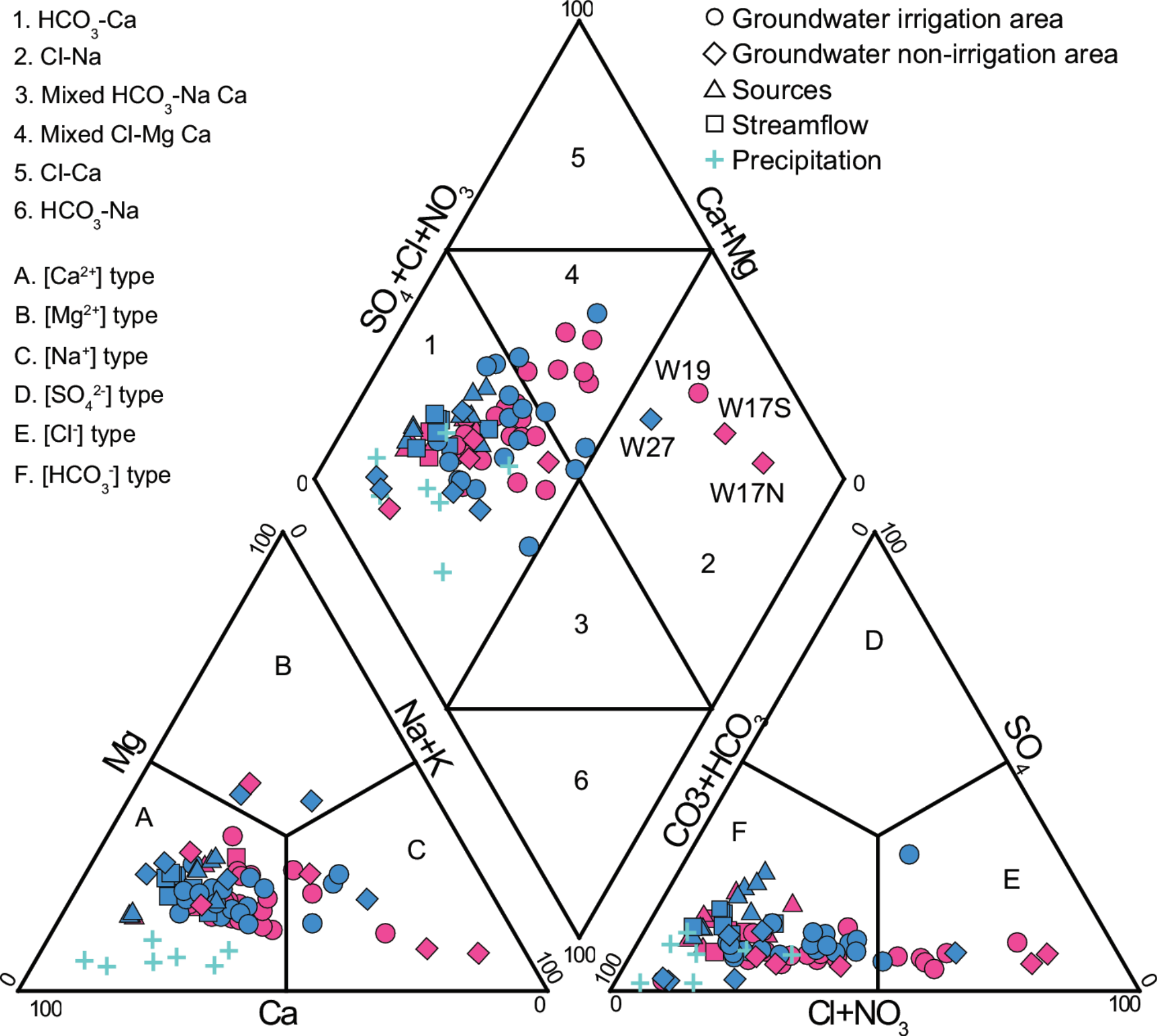
1. HCO3-Ca
2. Cl-Na
3. Mixed HCO3-Na Ca
4. Mixed Cl-Mg Ca
5. Cl-Ca
6. HCO3-Na
A. [Ca2+] type
B. [Mg2+] type
C. [Na+] type
D. [SO42-] type
E. [Cl-] type
F. [HCO3-] type
Groundwater irrigation area
Groundwater non-irrigation area
Sources
Streamflow
Precipitation
SO4+Cl+NO3
Ca+Mg
CO3+HCO3
Na+K
Mg
Ca
Cl+NO3
SO4
W19
W17S
W27
W17N
100
0

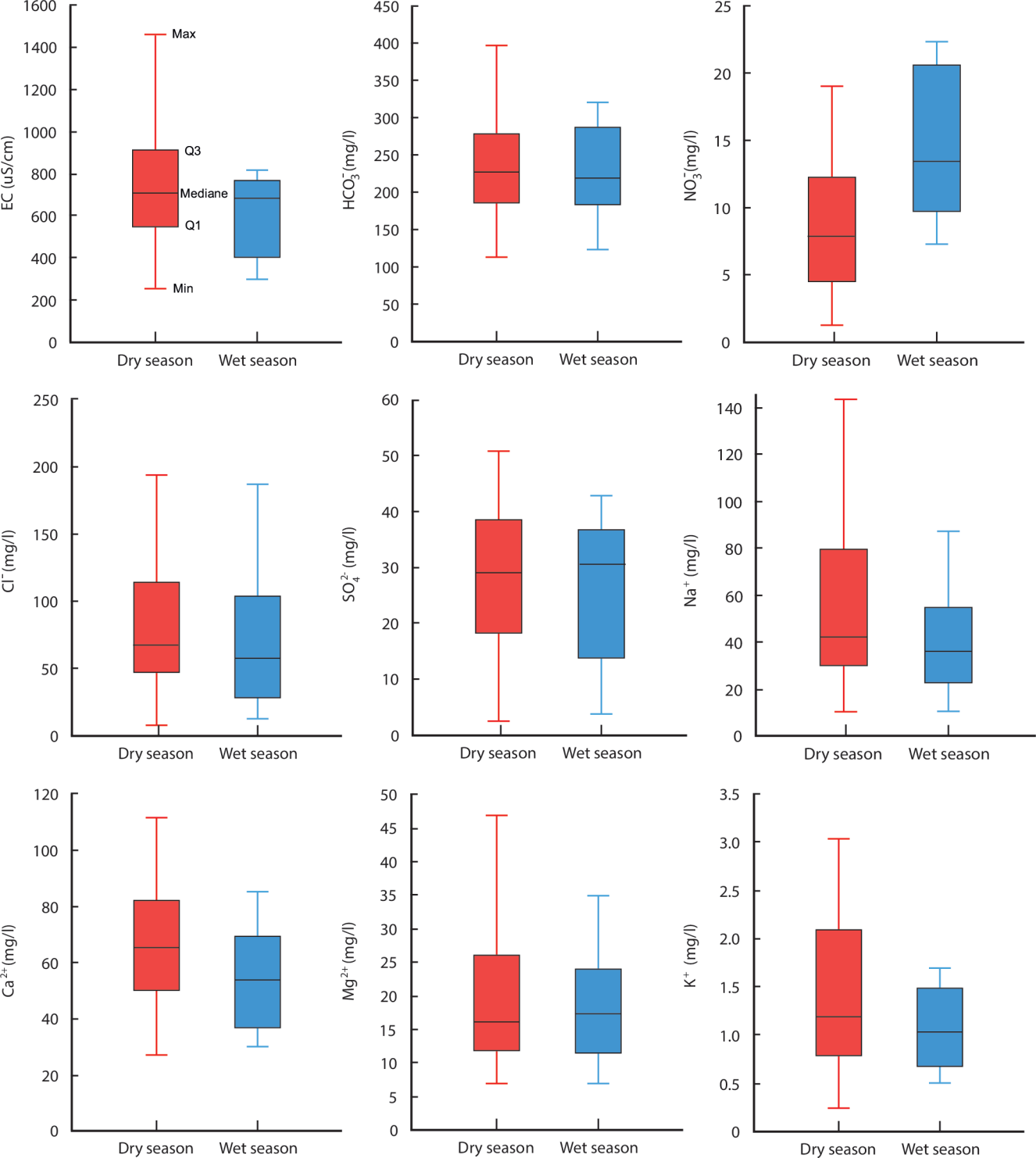
EC (uS/cm)
Max
Q3
Mediane
Q1
Min
Dry season
Wet season
HCO_3^-(mg/l)
NO_3^-(mg/l)
Cl^-(mg/l)
SO_4^{2-} (mg/l)
Na^+ (mg/l)
Ca^{2+}(mg/l)
Mg^{2+} (mg/l)
K^+ (mg/l)

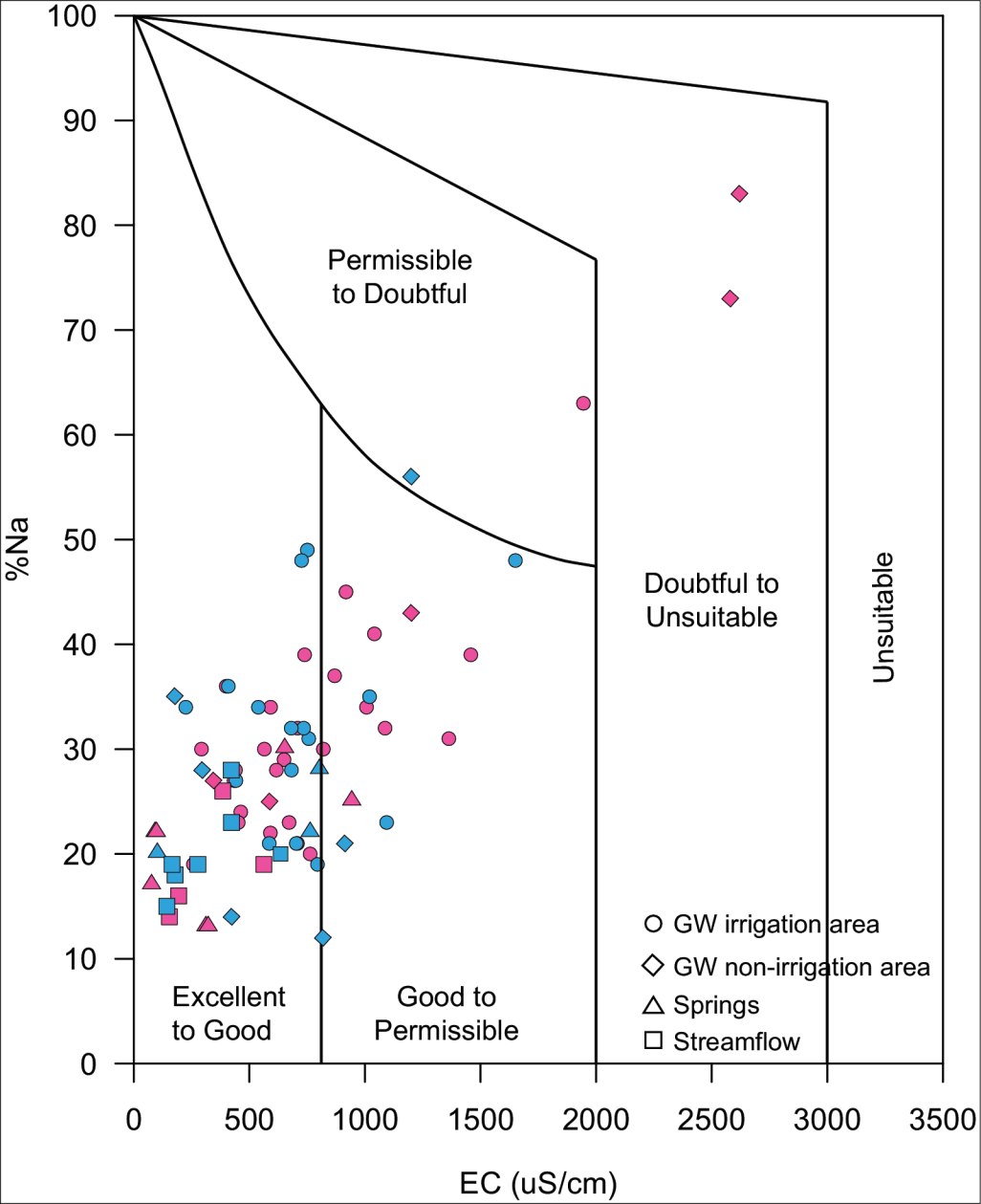
%Na
EC (uS/cm)
Permissible
to Doubtful
Doubtful to
Unsuitable
Unsuitable
Excellent
to Good
Good to
Permissible
GW irrigation area
GW non-irrigation area
Springs
Streamflow

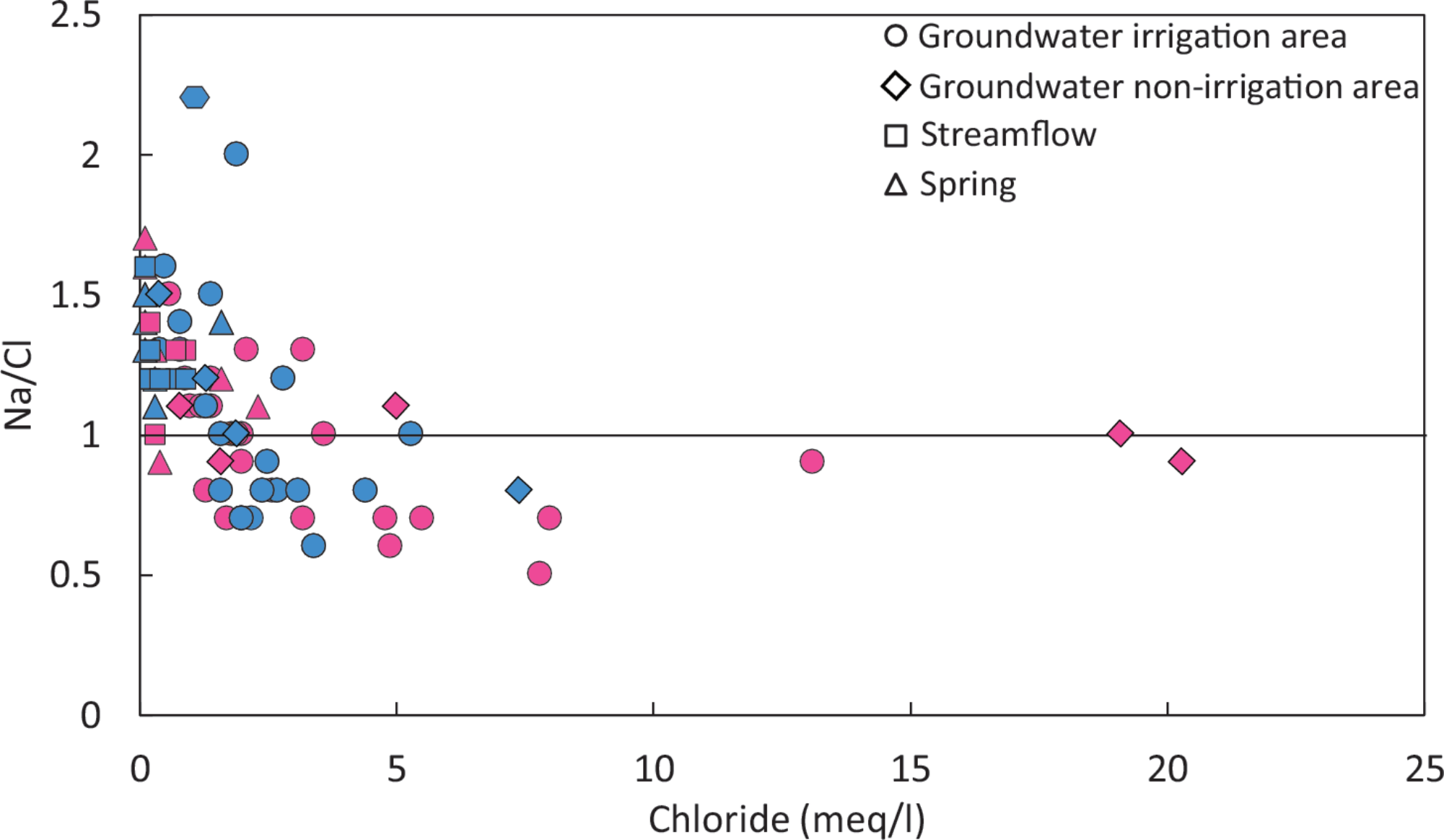
Groundwater irrigation area
Groundwater non-irrigation area
Streamflow
Spring
Na/Cl
Chloride (meq/l)
2.5
2
1.5
1
0.5
0
0
5
10
15
20
25

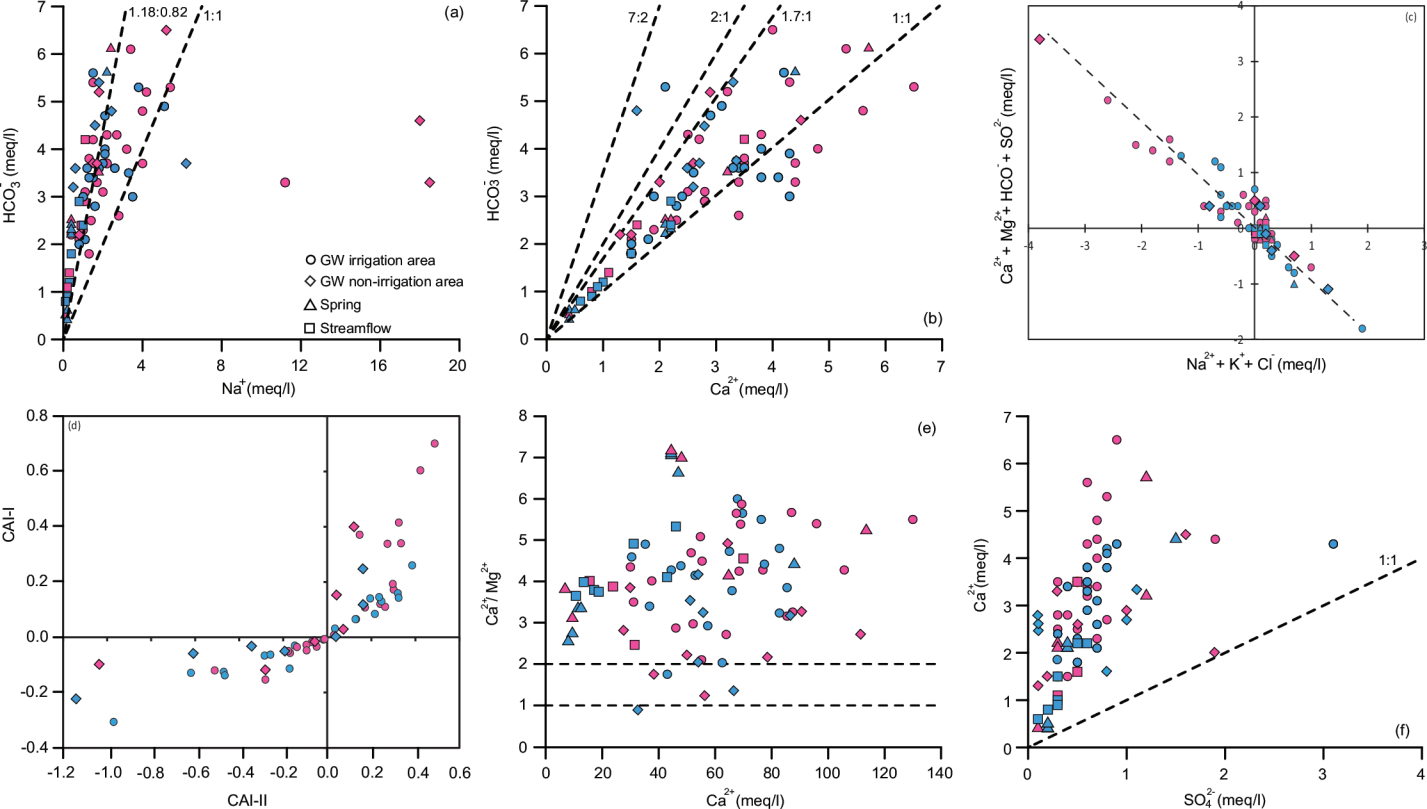
(a)
1.18:0.82
1:1
HCO3- (meq/l)
Na+ (meq/l)
GW irrigation area
GW non-irrigation area
Spring
Streamflow
(b)
7:2
2:1
1.7:1
1:1
HCO3- (meq/l)
Ca2+ (meq/l)
(c)
Ca2+ + Mg2+ + HCO- + SO2- (meq/l)
Na2+ + K+ + Cl- (meq/l)
(d)
CAI-I
CAI-II
(e)
Ca2+/ Mg2+
Ca2+ (meq/l)
(f)
1:1
Ca2+(meq/l)
SO4 2- (meq/l)

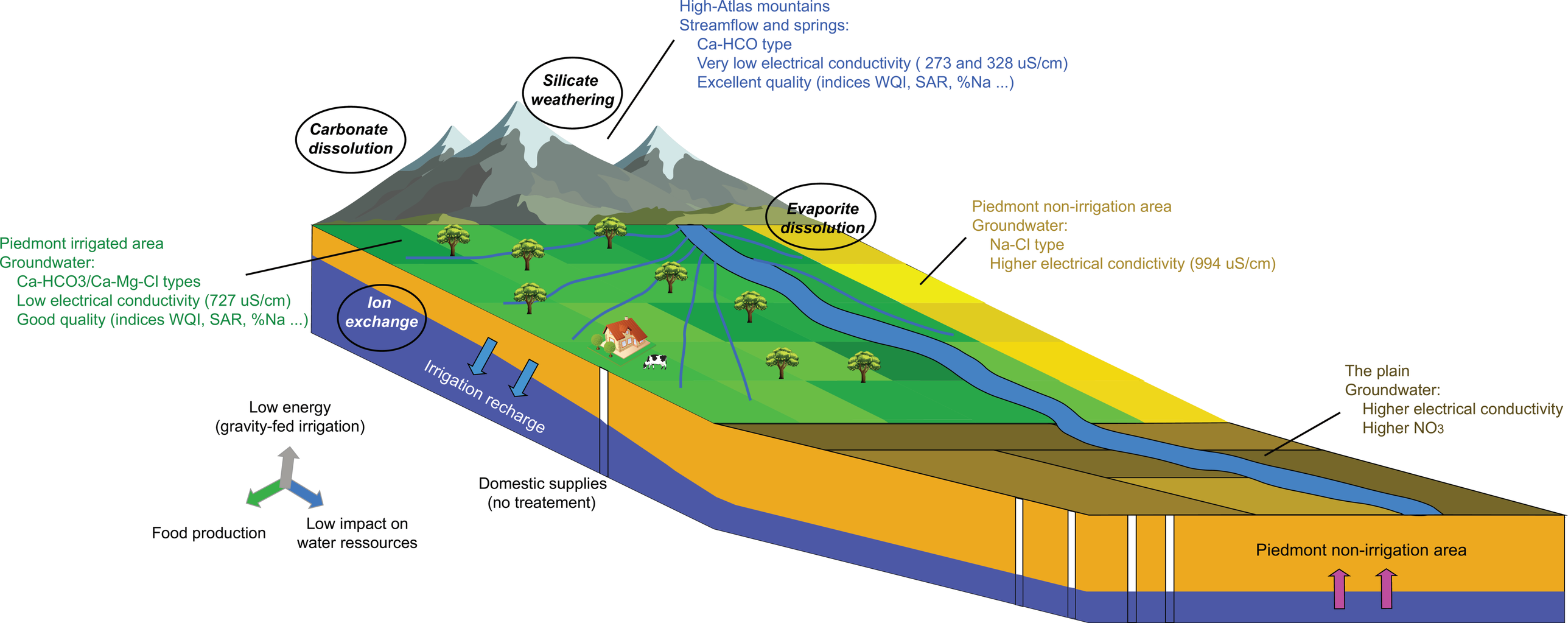
High-Atlas mountains
Streamflow and springs:
Ca-HCO type
Very low electrical conductivity (273 and 328 uS/cm)
Excellent quality (indices WQI, SAR, %Na ...)
Silicate weathering
Carbonate dissolution
Evaporite dissolution
Piedmont non-irrigation area
Groundwater:
Na-Cl type
Higher electrical condictivity (994 uS/cm)
Piedmont irrigated area
Groundwater:
Ca-HCO3/Ca-Mg-Cl types
Low electrical conductivity (727 uS/cm)
Good quality (indices WQI, SAR, %Na ...)
Ion exchange
Irrigation recharge
The plain
Groundwater:
Higher electrical conductivity
Higher NO3
Low energy
(gravity-fed irrigation)
Domestic supplies
(no treatement)
Food production
Low impact on
water ressources
Piedmont non-irrigation area